Preprint of: Mąkinia J., Mehrani M., Kowal P., Sobotka D., Godzieba M., Ciesielski S., Guo J., The coexistence and competition of canonical and comammox nitrite oxidizing bacteria in a nitrifying activated sludge system – Experimental observations and simulation studies, SCIENCE OF THE TOTAL ENVIRONMENT Vol. 864 (2023), 161084, DOI: 10.1016/j.scitotenv.2022.161084

# The coexistence and competition of canonical and comammox nitrite oxidizing bacteria in a nitrifying activated sludge system – experimental observations and simulation studies

**Mohamad-Javad Mehrani [1], Przemyslaw Kowal[1], Dominika Sobotka[1], Martyna Godzieba[2], Slawomir Ciesielski [2], Jianhua Guo[3], Jacek Makinia[1*]**

[1] Faculty of Civil and Environmental Engineering, Gdansk University of Technology, Narutowicza Street 11/12, 80-233 Gdansk, Poland

[2] Department of Environmental Biotechnology, Department of Environmental Biotechnology, University of Warmia and Mazury in Olsztyn, Sloneczna 45G, 10-719 Olsztyn, Poland

[3]Australian Centre for Water and Environmental Biotechnology (ACWEB, formerly AWMC), The University of Queensland, St. Lucia, Queensland 4072, Australia

*Correspondence: Jacek Makinia (Email: jmakinia@pg.edu.pl, Tel: +48 58 347 19 54, Address: Gdansk University of Technology, ul. Narutowicza 11/12, 80-233, Gdansk, Poland)

## Abstract

The second step of nitrification can be mediated by nitrite oxidizing bacteria (NOB), i.e. *Nitrospira* and *Nitrobacter*, with different characteristics in terms of the r/K theory. In this study, an activated sludge model was developed to account for competition between two groups of canonical NOB and comammox bacteria. Heterotrophic denitrification on soluble microbial products was also incorporated into the model. Four 5-week washout trials were carried out at dissolved oxygen-limited conditions for different temperatures (12°C vs. 20°C) and main substrates ($NH_4^+$-N vs. $NO_2^-$-N). Due to the aggressive reduction of solids retention time (from 4 to 1 d), the biomass concentrations were continuously decreased and stabilized after two weeks at a level below 400 mg/L. The collected experimental data (N species, biomass concentrations, and microbiological analyses) were used for model calibration and validation. In addition to the standard predictions (N species and biomass), the newly developed model also accurately predicted two microbiological indicators, including the relative abundance of comammox

bacteria as well as nitrifiers to heterotrophs ratio. Sankey diagrams revealed that the relative contributions of specific microbial groups to N conversion pathways were significantly shifted during the trial. The contribution of comammox did not exceed 5% in the experiments with both $NH_4^+$-N and $NO_2^-$-N substrates. This study contributes to a better understanding of the novel autotrophic N removal processes (e.g. deammonification) with nitrite as a central intermediate product.

***Keywords***: Process Simulation; Comammox; *Nitrospira*; *Nitrobacter*; Two-step nitrification

## 1. INTRODUCTION

Although nitrification has been known since the end of the 19th century, the process of understanding has changed dramatically in recent 30 years, which was reflected by evolving descriptions in the Metcalf and Eddy handbook series (1990, 2003, 2014). The second stage of nitrification (nitrite oxidation, nitratation) has been receiving special attention in response to the development of the novel shortcut nitrogen (N) removal processes, including deammonification and a shortened pathway of nitrification-denitrification via nitrite ("nitrite shunt"). In those processes, nitrite is a central component and effective suppression of nitrite oxidizing bacteria (NOB) is required for successful performance. However, the knowledge of the metabolism of NOB has been limited and NOB remains a "big unknown of the nitrogen cycle" (Daims et al., 2016).

Traditionally, the genus *Nitrobacter* was considered the typical NOB representative (Metcalf and Eddy, 1990), whereas more recently the genus *Nitrospira* has been accepted as a more common NOB population (Metcalf and Eddy, 2014). The dominance of *Nitrospira* in the NOB population of activated sludge systems has indeed been confirmed in numerous recent laboratory- and full-scale studies (Keene et al., 2017; Li et al., 2020; Persson et al., 2017; Wu et al., 2019; Zheng et al., 2019a). Mehrani et al., (2020) presented a comprehensive review study and meta-analysis on the role of *Nitrospira* in the N removal systems.

These two genera (*Nitrobacter* and *Nitrospira*) reveal different characteristics in terms of the r/K theory. *Nitrobacter* represents the r-strategists which grow faster at high concentrations of the substrates ($NO_2^-$-N and dissolved oxygen (DO)), whereas *Nitrospira* is the K-strategist with high substrate affinity at low concentration (Yu et al., 2020). Due to these differences, a more complex

suppression strategy would be required for NOB. In general, the controlled solids retention time (SRT), combined with DO-limited conditions and high residual ammonia, have been recommended (Regmi et al., 2014). However, low DO conditions (<1.0 mg $O_2$/L) can be inefficient with respect to the suppression of K-strategist *Nitrospira* (Cao et al., 2017).

In addition to the competition between *Nitrobacter* and *Nitrospira*, recent findings suggest that there are other critical issues to be considered for NOB suppression. These issues comprise the occurrence of different NOB populations, such as *Ca. Nitrotoga* (Kitzinger et al. 2018) and specific metabolic properties of some microorganisms, such as comammox-*Nitrospira*. In particular, the discovery of comammox, i.e. complete ammonia oxidation, by a single *Nitrospira*-type microorganism (Daims et al., 2015; van Kessel et al., 2015) has overturned "a century-old dogma of nitrification research" (Koch et al., 2019). However, the actual role of comammox bacteria in full-scale WWTPs is still ambiguous (Koch et al., 2019).

The dominance of specific groups of nitrifying bacteria results from selective pressures of the operational conditions in the bioreactor, including substrate ($NH_4^+$-N or $NO_2^-$N) concentration, DO concentration, and temperature (Metcalf and Eddy, 2014). An efficient approach to the investigation of the complex nitrifier competition would be a combination of dedicated physical experiments with advanced microbiological analyses and mathematical modeling. Cao et al. (2017) noted that the nitrification models should accommodate appropriately the competition between AOB and NOB to understand factors influencing the competition between autotrophic N-converting organisms. Two-step nitrification models have been continuously developed for almost 60 years as summarized by (Mehrani et al., 2022). Such models were used for the development of suppression strategies for NOB considered collectively as one group (Duan et al.,

2019; Kent et al., 2019; Ma et al., 2017; Pérez et al., 2014). Very recent theoretical advances include the examination of the competition for different r/K strategist groups of AOB and NOB (Yu et al., 2020; Yin et al., 2022) and the incorporation of comammox in the traditional two-step model (Mehrani et al., 2021). However, no models have been applied in practice to investigate the competition of different NOB groups under different substrate (limited vs. unlimited) conditions.

The purpose of this study was to develop and validate a model describing the co-existence and competition between comammox NOB and two groups of canonical NOB, termed NOB1 (*Nitrospira*) and NOB2 (*Nitrobacter*), revealing different r/K characteristics, in response to decreasing SRTs under different substrate limitation conditions. The experimental data were collected during four long-term washout experiments carried out at two temperatures (12°C vs. 20°C) with different substrates ($NH_4^+$-N vs. $NO2^-$- N). The effect of the substrate was also investigated in terms of the behavior of comammox bacteria. Overall, it was hypothesized that the newly developed model would provide a better explanation of the competition between the different NOB groups. Such a model can be a diagnosis and optimization tool for practical applications of the novel shortcut N removal processes under different $NO_2^-$-N availabilities.

## 2. MATERIAL AND METHODS

### 2.1. Laboratory experiments and data collection for modeling

#### *2.1.1. Long-term washout experiments with different nitrogen substrates*

Four long-term washout trials were carried out under various laboratory conditions concerning the nitrogen substrate and temperature (Table 1). For each experiment, new inoculum biomass samples were obtained from a large municipal wastewater treatment plant (WWTP) in Swarzewo (180 000 PE), located in northern Poland. The biological part of that plant, performing biological nutrient removal, consists of six parallel sequencing batch reactors (SBRs). The effluent standards have been set following the European Union Urban Wastewater Directive (91/21/EEC), i.e., total N (TN) = 10 mg N/L and total P (TP) = 1 mg P/L.

The laboratory experiments were carried out in a fully automated plexiglass SBR with a working volume of 10 L. The reactor was placed in a thermostatic water bath to keep the temperature setpoints. Control systems were also installed for aeration and pH. A detailed description of the laboratory setup can be found elsewhere (Mehrani et al., 2022).

In each experiment, the reactor was operated at three cycles per day (8 hours each), including three phases: feeding (15 minutes), reaction (450 minutes), and decantation (15 minutes). The latter phase was carried out while mixing, so the solids retention time (SRT) became equal to the hydraulic retention time. The amount of waste activated sludge (WAS), removed during the decantation phase, was progressively increasing. This resulted in a gradually decreasing SRT from the initial 4 d to 1 d at the end of the trial. For all the experiments, the continuous aeration mode was employed with the DO setpoint of 0.6±0.1 mg/L, while the pH was kept at 7.5±0.2 by dosing NaOH (2M solution). The temperature setpoints were kept close to the actual process

conditions, i.e., 12ºC (winter) and 20ºC (summer). For a better understanding of the competition between the NOB groups, the reactor was fed with either $NH_4^+$-N or $NO_2^-$-N as the sole inorganic N substrate. The influent N loadings and detailed feed composition are shown in the SI (Figure S1 and Table S1, respectively).

Mixed liquor samples were collected 3 times per week, then filtered and analyzed for different N forms, including $NH_4^+$-N, $NO_3^-$-N, and $NO_2^-$-N, at the initial and the end of the reaction phase. Mixed liquor suspended solids (MLSS) and mixed liquor volatile suspended solids (MLVSS) concentrations were analyzed at the initial of the reaction phase. For microbiological analyses, biomass samples were collected from the reactor in duplicate three times: at the beginning (0 d), in the middle phase (20 d), and at the end of each trial (35 d). The samples from the initial and middle phases were transferred to 50 mL Falcon-type tubes for sedimentation and thickening. The terminal samples, due to the dilution of mixed liquor, were obtained by filtering 5 L of the effluent through 0.22 μm pore size filters. The biomass samples were stored at -25°C prior to DNA extraction.

**Table 1.** Operational parameters and conditions in the reactor during the washout experiments

| Trial | Temperature (˚C) | pH | DO (mg $O_2$/L) | Source of N in the feed | MLSS/MLVSS (mg/L) |
|---|---|---|---|---|---|
| T1 | 20 | 7.5±0.2 | 0.6±0.1 | $NH_4^+$-N | 2140/1500 |
| T2 | 12 | 7.5±0.2 | 0.6±0.1 | $NH_4^+$-N | 1890/1450 |
| T3 | 20 | 7.5±0.2 | 0.6±0.1 | $NO_2^-$-N | 1970/1520 |
| T4 | 12 | 7.5±0.2 | 0.6±0.1 | $NO_2^-$-N | 2020/1440 |

### *2.1.2. Chemical and microbiological analytical methods*

The analytical methods used by Dr. Lange and Shimadzu were based on the APHA Standard Methods (2002). Cuvette tests in a Xion 500 spectrophotometer were used to determine $NH_4^+$-N, $NO_3^-$-N, and $NO_2^-$-N concentrations (Hach Lange, Germany). Before the analysis, mixed liquor samples were filtered under vacuum pressure using a 1.2 m pore size nitrocellulose filter MFV-3 (Millipore, USA). The gravimetric technique was used to determine the MLSS concentration and its volatile fraction (MLVSS) in line with the APHA Standard Methods (2002).

The DNA extraction was performed followed by FastDNA™ SPIN KIT (MP Biomedicals, USA) based on the manufacturer's manual. Genomic DNA extracted from the duplicated samples was pooled together. Following purification, the DNA was utilized for the Illumina Next Generation Sequencing procedure. Similar to our previous studies (Al-Hazmi et al., 2021), high-throughput Illumina sequencing of the V3-V4 regions of the 16S rRNA gene procedure and subsequent DNA sequencing data processing and analysis were carried out.

## 2.2. Organization of the modeling study

The whole modeling study was arranged in five steps as shown in Figure 1, and each step was described in the following sub-sections.

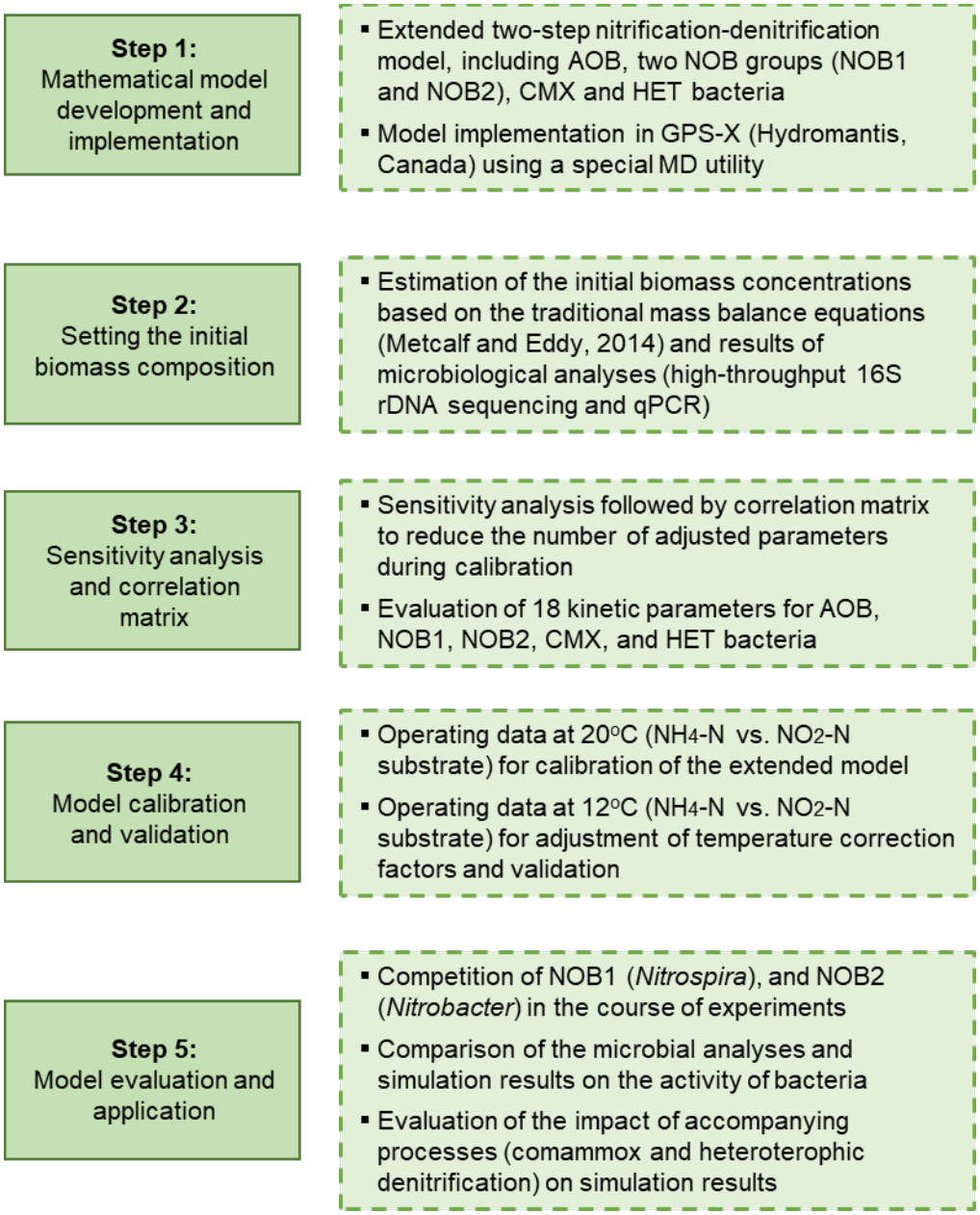


**Figure 1.** Flowchart diagram of the simulation procedure and model application for the competition of two NOB groups and interactions with comammox and heterotrophic denitrification

### *2.2.1. Mathematical model development and implementation*

The microbial growth model, used in the present study, was based on the death-regeneration concept from the Activated Sludge Model No. 1 (ASM1) (Henze, 2000). In our previous studies, a two-step nitrification model was developed with further expansions to incorporate comammox (Mehrani et al., 2021) and heterotrophic denitrification on soluble microbial products (SMP)

(Mehrani et al., 2022). In the present study, NOB were divided into two subgroups depending on their different characteristics in terms of the r/K theory, i.e., *Nitrospira* as K-strategists vs. *Nitrobacter* as r-strategists (Figure 2b). Their behavior and competition were assessed during the washout experiments under different substrate availabilities (Table 2). It was assumed that the substrate affinity is higher for *Nitrobacter* than *Nitrospira* ($K_{NO2,NB} > K_{NO2,NS}$) allowing the latter to prevail under $NO_2^-$-N limited conditions ($NH_4^+$-N feeding). On the other hand, *Nitrobacter* can outcompete *Nitrospira* under $NO_2^-$-N feeding due to a higher maximum specific growth rate ($\mu_{max,NB} > \mu_{max,NS}$).

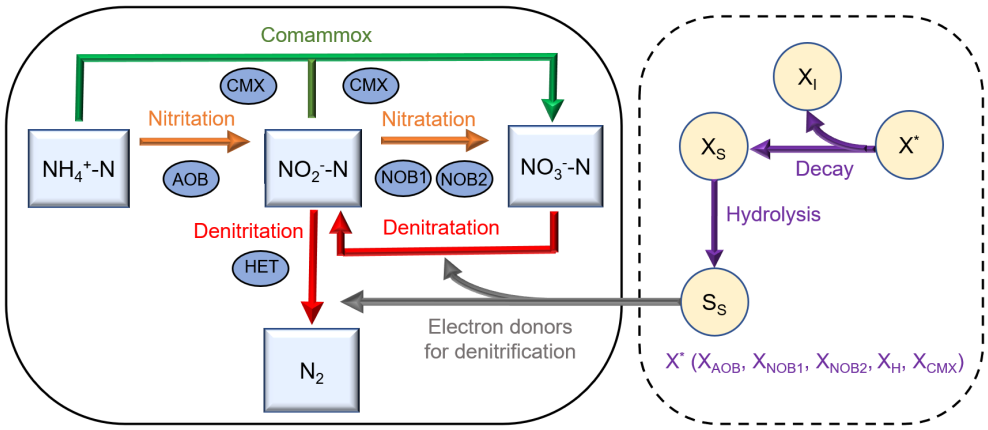


**Figure 2.** A concept of the extended nitrification model considering two NOB groups and interactions with comammox and heterotrophic denitrification

The GPS-X software 8.0 (Hydromantis, Canada) was used as a simulation environment for implementing the model and running simulations. Internal GPS-X utilities were used for sensitivity analysis (Analyzer) and parameter optimization (Optimizer).

**Table 2.** Effect of the substrate conditions (limited vs. unlimited) on the different r/K NOB strategists

| NOB substrate availability | *Nitrospira* (K-strategist) | *Nitrobacter* (r-strategist) |
|---|---|---|
| Limited ($NH_4^+$-N feed) | ↑ $\mu_{max,NS}\frac{S_{NO2}}{S_{NO2}+\mathbf{K_{NO2,NS}}}\frac{S_O}{S_O+K_{O,NS}}$ | ↓ $\mu_{max,NB}\frac{S_{NO2}}{S_{NO2}+K_{NO2,NB}}\frac{S_O}{S_O+K_{O,NB}}$ |
| Unlimited ($NO_2^-$-N feed) | ↓ $\mu_{max,NS}\frac{S_{NO2}}{S_{NO2}+K_{NO2,NS}}\frac{S_O}{S_O+K_{O,NS}}$ | ↑ $\boldsymbol{\mu_{max,NB}}\frac{S_{NO2}}{S_{NO2}+K_{NO2,NB}}\frac{S_O}{S_O+K_{O,NB}}$ |

### *2.2.2. Setting the initial conditions (biomass composition and model parameters)*

The mechanistic ASM-type models require a setting of the initial concentrations for specific groups of microorganisms. Based on the systematic protocol proposed in the previous study (Mehrani et al., 2022), a combination of mass balance calculations and microbiological analyses were applied to determine the initial concentrations of AOB, NOB (*Nitrospira*), comammox bacteria, and denitrifying heterotrophs. The abundances of *Nitrobacter* were below the detection limit in all the initial samples. Therefore, the initial concentrations of these bacteria were set at 1% of *Nitrospira* initial concentration.

The initial values of kinetic and stoichiometric parameters were adopted from the literature (Koch et al., 2019; Yu et al., 2020; Metcalf and Eddy 2003; Hiatt and Grady, 2008; Roots et al. 2019). Subsequently, the kinetic parameters were subjected to sensitivity analysis (see Section 2.3). Three kinetic parameters, including $K_O$ for AOB and NOB1 together with $K_{NO2}$ for NOB1, were experimentally determined in batch tests (Mehrani et al., 2022). These parameters were not further adjusted during model calibration.

## 2.3. Sensitivity analysis and correlation matrix

Coupling local sensitivity analysis and the development of a correlation matrix allows reducing the number of parameters adjusted during model calibration. The analysis was carried out based on the results from trial T1 ($NH_4^+$-N substrate) and trial T3 ($NO_2^-$N substrate). For trial T1, the different microbial groups (AOB, NOB1, CMX, and HET) were subjected to the sensitivity analysis concerning $NH_4^+$-N, $NO_3^-$N, and $NO_2^-$N behavior. In trial T3, AOB were not considered due to the lack of substrate ($NH_4^+$-N) for these bacteria. Instead, NOB2 were included concerning $NO_3^-$N and $NO_2^-$N behavior. The classification of sensitivity coefficients, $S_{i,j}$, (from 0 to >2.5) was adopted from a recent study of Cao et al. (2020).

Subsequently, all pairs of the most sensitive kinetic parameters were evaluated by the correlation matrix. If the correlation coefficient for any pair is high enough, the calibration procedure can be simplified by adjusting only one of the two parameters (Zhu et al., 2015).

## 2.4. Model calibration and validation

The results of the trials at 20 ℃ (T1 and T3) with both substrates ($NH_4^+$-N vs. $NO_2^-$-N) were used for model calibration, while the results of the two trials at 12 ℃ (T2 and T4) were used for validation. The Nelder-Mead simplex method with the maximum likelihood objective function was used for parameter estimation as described in detail in a previous study (Lu et al. 2019). The model efficiency was assessed using the conventional performance metrics, such as the determination coefficient ($R^2$), root mean square error (RMSE), and mean absolute error (MAE). In addition, the Janus coefficient ($J^2$) was calculated to evaluate a change in the model efficiency between the calibration and validation phases (Hauduc et al., 2015).

### 2.5. Model evaluation and application

After model validation, the competition between two NOB groups (*Nitrospira* and *Nitrobacter*) under different substrate conditions ($NH_4^+$-N and $NO_2^-$N) was investigated by comparing the predicted process rates (mg N/L·d) in trials T1 and T3. Sankey diagrams were developed based on the daily average rates at different phases of the experiment, i.e. 0 d (beginning), 20 d, and 35 d (end). The diagrams were used to identify the dominant N conversion pathways and assess the effect of the accompanying processes (comammox, heterotrophic denitrification).

## 3. RESULTS

### 3.1. Initial biomass composition

In all the trials, the initial MLSS and MLVSS concentrations were approximately 2000 and 1500 mg/L, respectively (Table 1). The calculated initial concentrations of the specific microbial groups ($X_{AOB}$, $X_{NOB}$, $X_{CMX}$, $X_{HET}$), estimated sequentially using the systematic protocol of Mehrani et al. (2022), are shown in the SI (Table S3).

### 3.2. Sensitivity analysis and correlation matrix

Figure 3a,c shows the sensitivity coefficients, derived for all 18 kinetic coefficients (μ, K, b), which were obtained based on the results from trial T1 ($NH_4^+$-N substrate) and trial T3 ($NO_2^-$N substrate). For trial T1, the different microbial groups (AOB, NOB1, CMX, and HET) were subjected to the sensitivity analysis for the behavior of $NH_4^+$-N, $NO_3^-$N, and $NO_2^-$N. For trial T3, NOB2 were considered instead of AOB, and the sensitivity analysis was performed based on the behavior of $NO_3^-$N and $NO_2^-$N.

In general, for trial T1, the very influential coefficients *($S_{i,j} \geq 2$)* were $\mu_{AOB}$ and $\mu_{NOB1}$ concerning the behavior of $NO_2^-$N, and $\mu_{NOB1}$ associated with the behavior of $NO_3^-$N. The $\mu_{AOB}$ had also a substantial influence *($1 \leq S_{i,j} < 2$)* on the behavior of $NH_4^+$-N, while $\mu_{CMX}$ was very influential *($S_{i,j} \geq 2$)* on the $NO_3^-$N behavior. The decay rates ($b_{AOB}$ and $b_{NOB1}$) and DO half-saturation coefficients ($Ko_{AOB}$ and $Ko_{NOB1}$) were influential *($1 \leq S_{i,j} < 2$)* on the $NO_2^-$N behavior.

For trial T3, $\mu_{NOB1}$ and $\mu_{CMX}$ with $S_{i,j}>2$, followed by $\mu_{NOB2}$ with $S_{i,j} = 1.8$, were the most influential coefficients associated with the behavior of $NO_3^-$N. The decay rates ($b_{NOB1}$ and $b_{NOB2}$) were also influential *($S_{i,j}>1$)* with respect to the behavior of $NO_2^-$N and $NO_3^-$N.

Based on the results of sensitivity analysis for both trials, the very influential kinetic parameters ($S_{i,j}>1$) were subjected to evaluation by a correlation matrix (Figure 3b,d). In general, the highest correlation coefficients in both trials referred to the maximum growth rates (μ) and decay coefficients (b) for all the nitrifier groups. Hence, for simplification of the calibration procedure, b coefficients were omitted in further adjustments.

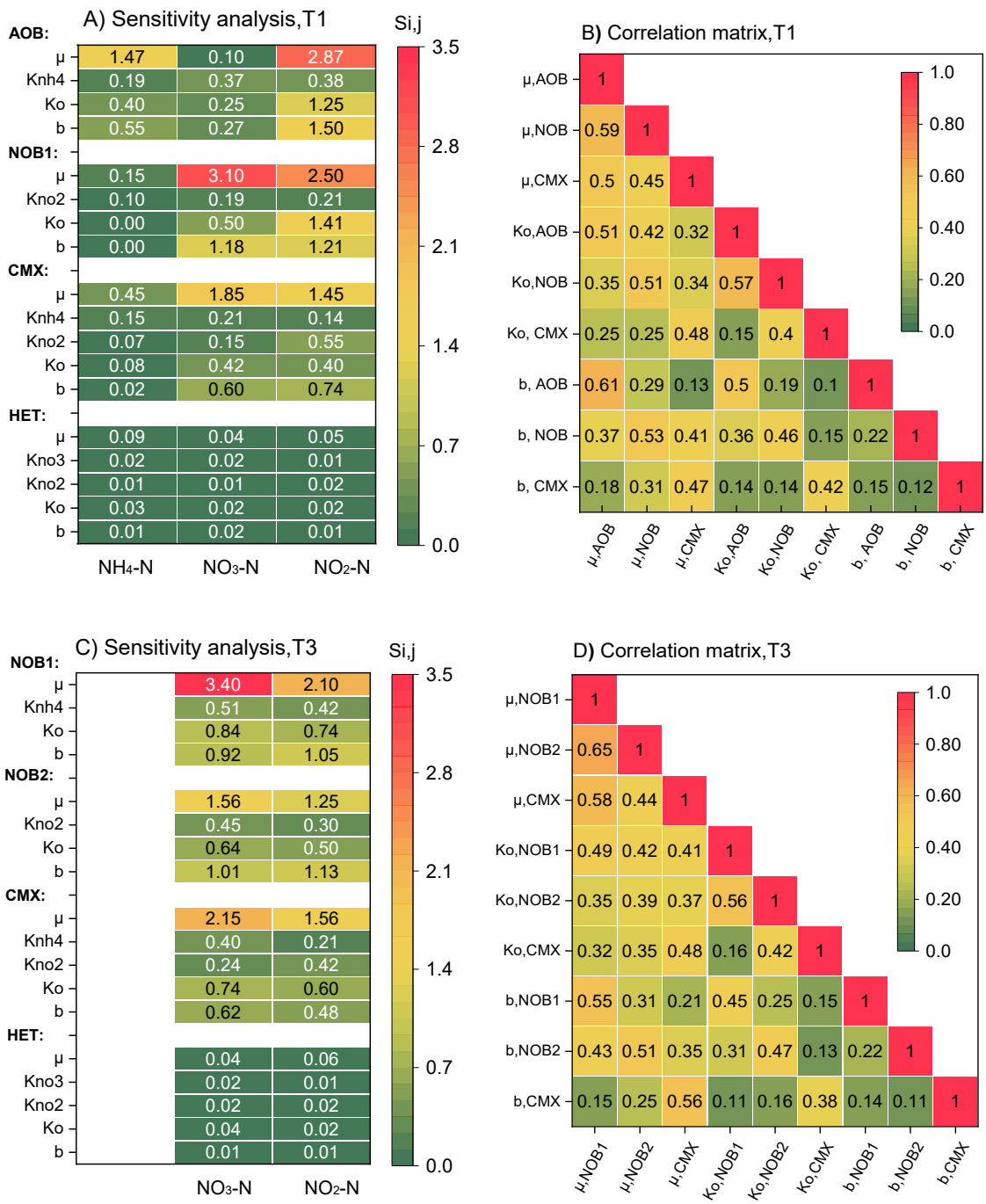


**Figure 3.** Sensitivity coefficients, $S_{i,j}$, and correlation matrix for the most sensitive kinetic parameters ($\mu$, K, b) in trial T1 (A-B) and trial T3 (C-D) (the effect of NOB2 in trial T1 was not considered due to very low sensitivity ($S_{i,j} \leq 0.01$))

### 3.3. Model calibration and validation

The experimental observations and predicted behaviors of N species ($NH_4^+$-N, $NO_3^-$N, and $NO_2^-$N), and biomass concentrations for the calibrated model (trials T1 and T3) are shown in Figure 4. Similar data for the validated model (trials T2 and T4) are shown in Figure 5. In all the trials, the biomass concentrations (MLSS, MLVSS) were continuously decreased and stabilized after two weeks at below 400 mg/L. Moreover, regardless of the substrate ($NH_4^+$-N vs. $NO_2^-$-N), the behavior of $NO_3^-$N was generally similar with a peak concentration occurring after one week.

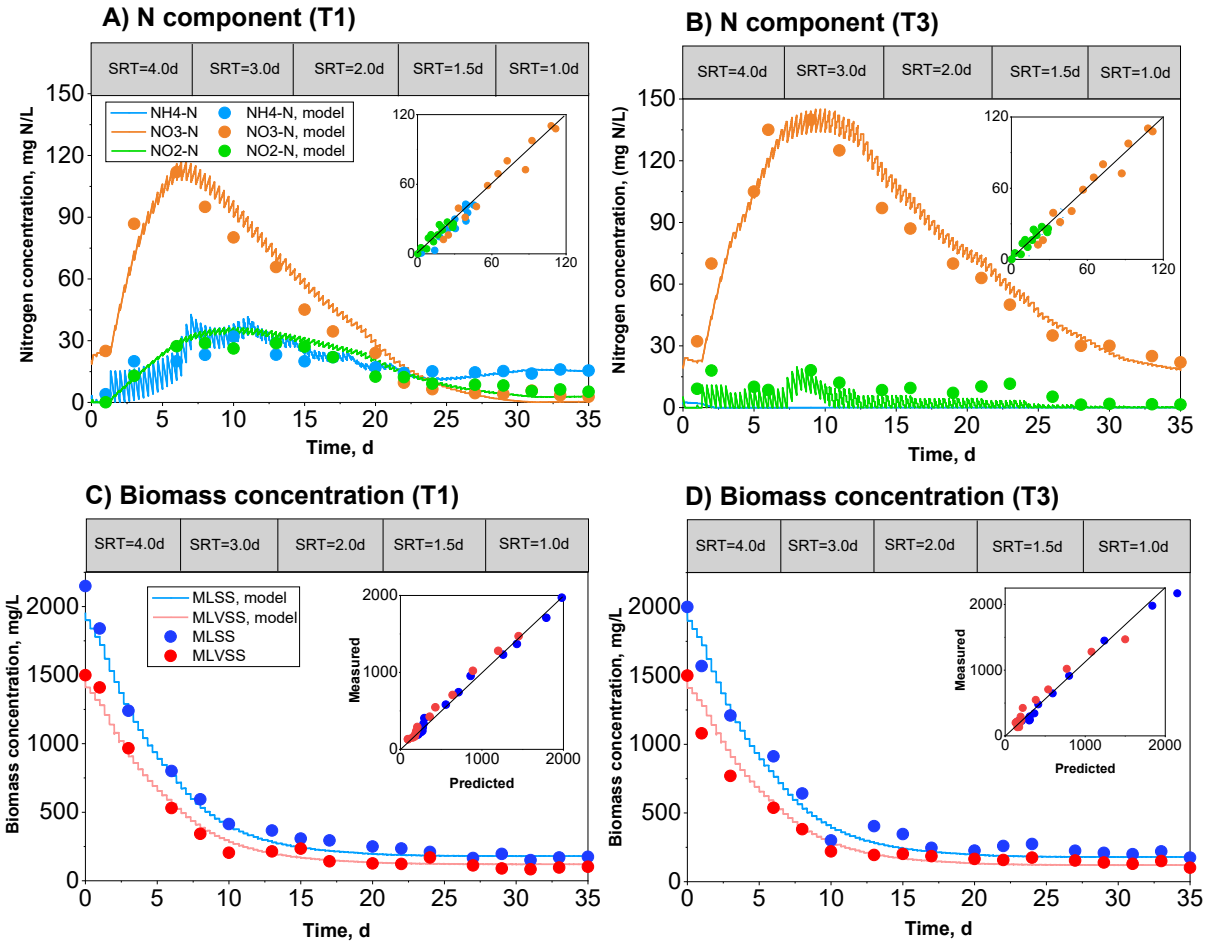


**Figure 4.** Observed data vs. model predictions for the calibrated model: A) N components in trial T1, B) N components in trial T3, C) Biomass concentrations in trial T1, D) Biomass concentrations in trial T3

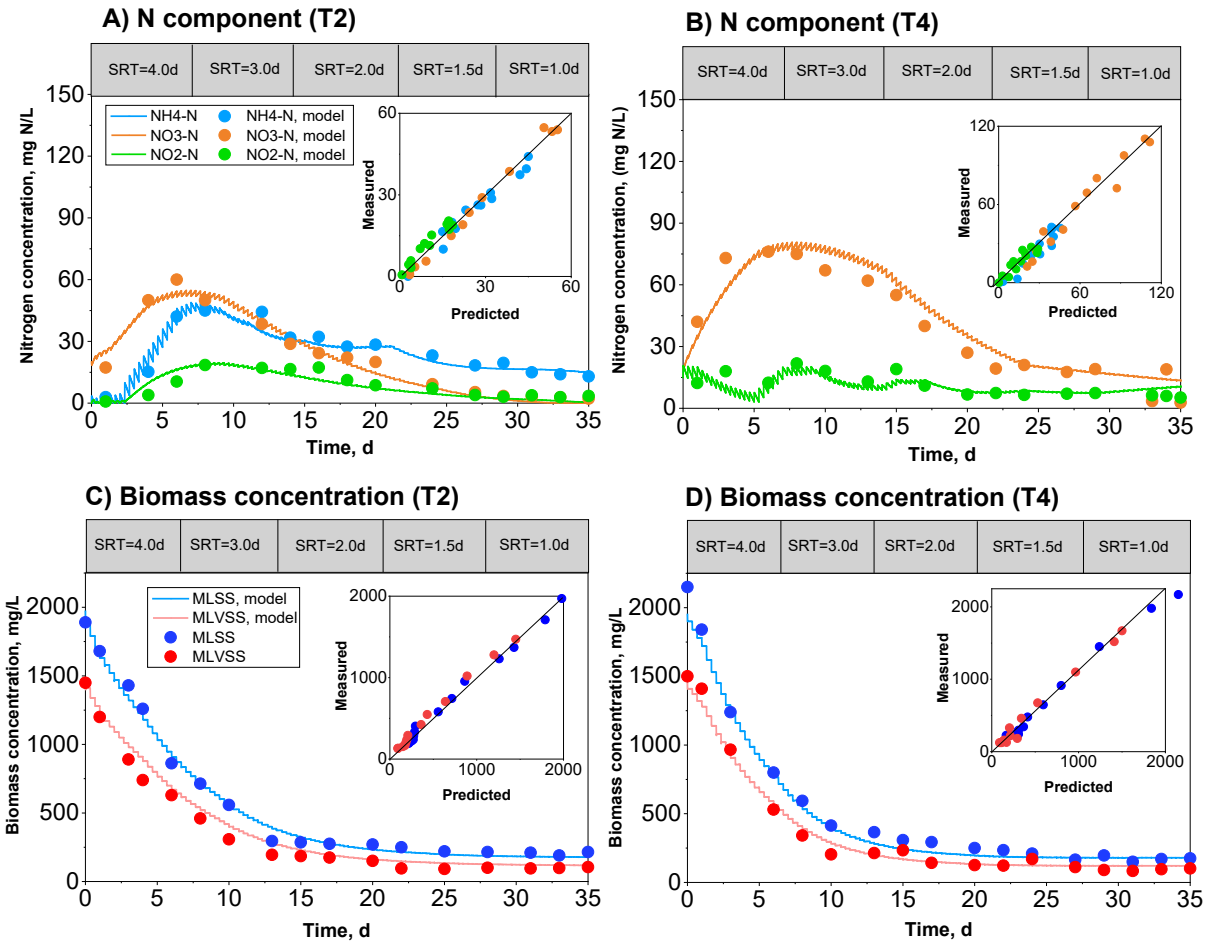


299

300 **Figure 5.** Observed data vs. model predictions for the validated model: A) N components in T2, B) N components

301 in T4, C) Biomass concentrations in T2, D) Biomass concentrations in T4

302

303 In addition to the standard predictions (N species and biomass), the newly developed model also

304 predicted two microbiological indicators, including the relative abundance of comammox

305 bacteria and nitrifiers (NIT) to heterotrophs (HET) ratio (Figure 6). The relative abundance of

306 comammox bacteria in the trials with $NH_4^+$-N substrate (T1 and T2) decreased and stabilized at

307 0.4-0.5 (Figure 6a-b), while in the trials with $NO_2^-$-N substrate (T3 and T4), the abundance

308 sharply decreased in the first week and stabilized at 0.1-0.2 at the end of trials (Figure 6c-d). The

309 results with $NO_2$—N substrate strongly suggest that comammox bacteria can grow on $NO_2$—N, as

310 the model predictions significantly worsened without considering that process (Figure 6c-d).

The NIT/HET ratios in trials T1 and T2 were stable at 0.1-0.15 at the beginning and middle phases and then decreased to 0.05 at the end of the trials (Figure 6e-f). In contrast, the NIT/HET ratios in trials T3 and T4 were relatively stable (0.04-0.05) at the beginning and middle phase, and then increased to >0.05 at the end of the trials (Figure 6g-h).

Table 3 shows a list of the model parameters along with their related values and sources of information. Due to high sensitivity ($S_{i,j} \geq 0.5$), the μ and Ko for all the nitrifier groups (AOB, NOB1, NOB2, CMX), and μ for heterotrophs were adjusted during mathematical optimization. The estimated values were further discussed in relation to literature data (see Section 4.1). The extended model prediction performance for each model output ($NH_4^+$-N, $NO_3^-$N, $NO_2^-$N) is presented in Table 4. The calibrated model exposed a high goodness-of-fit for all the outputs in terms of $R^2$ (>0.87) and RMSE and MAE errors (2.20-3.4), while the validated model revealed slightly decreased (<7%) $R^2$, and slightly increased (<15%) errors (RMSE, MAE) compared to the calibration period. The Janus coefficient varied in the range of 1.31-1.97, which also confirmed the model validity.

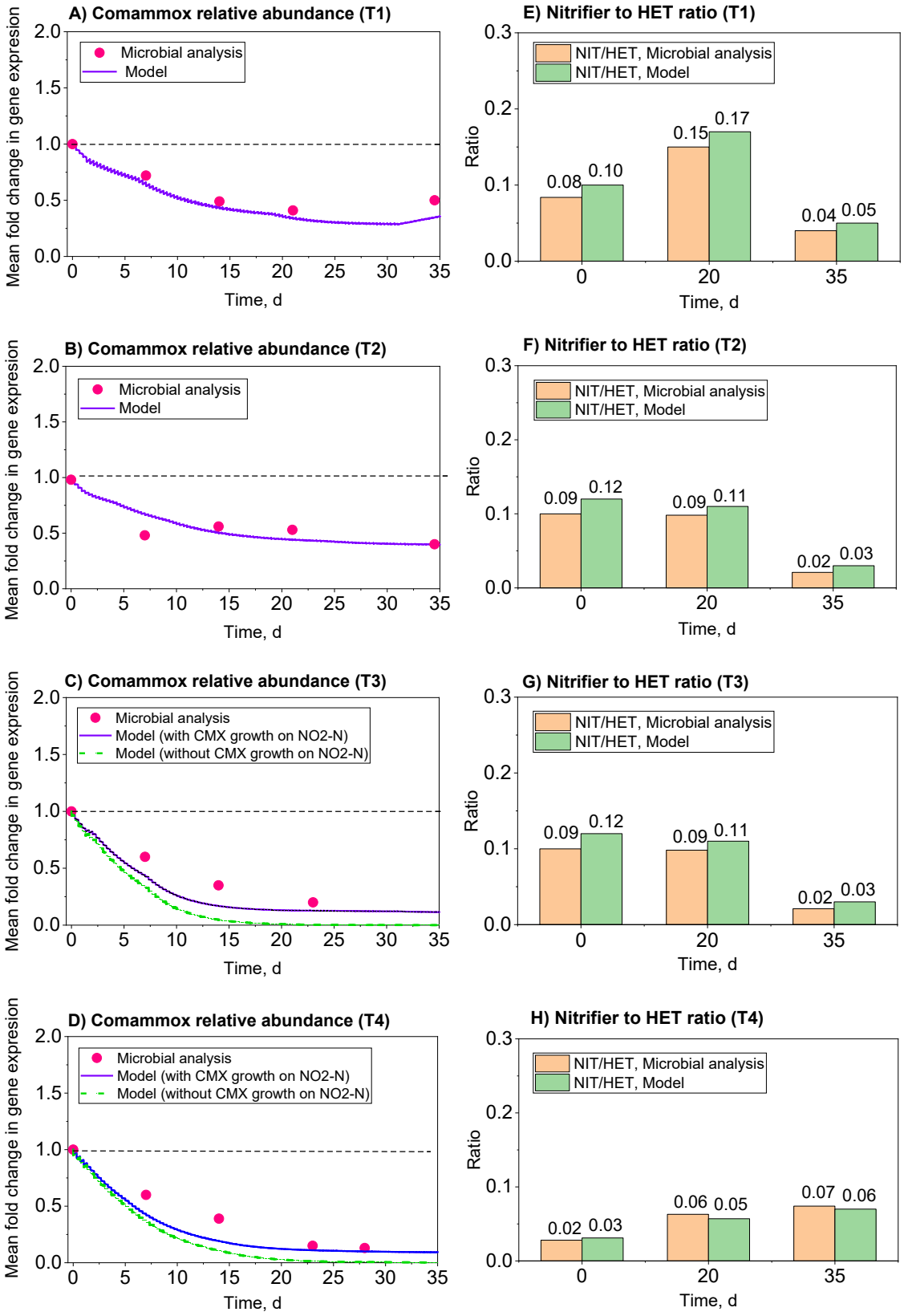


**Figure 6.** Observed vs. predicted relative adundances of comammox bacteria (A-D), and the ratio of nitrifiers to heterotrophs (E-H) for trials T1-T4

**Table 3**. List of the adjusted kinetic parameters during model calibration, their values and sources of information

| Parameter | Unit | Bacterial group | | | | | Source |
|---|---|---|---|---|---|---|---|
| | | AOB | NOB 1 | NOB 2 | CMX | HET | |
| | | | *Nitrospira* | *Nitrobacter* | | | |
| **Kinetic** | | | | | | | |
| $\mu$ | $d^{-1}$ | 0.38 | 0.21 | 0.60 | 0.20 | 1.00 | Optimization |
| $K_O$ | mg $O_2$/L | - | - | 0.45 | 0.30 | - | Optimization |
| $K_O$ | mg $O_2$/L | 0.17 | 0.13 | - | - | - | Experimental |
| $K_O$ | mg $O_2$/L | - | - | - | - | 0.20 [d] | Literature |
| $K_{NH4}$ | mg $NH_4$/L | 0.67[a] | - | - | 0.012[b] | - | Literature |
| $K_{NO2}$ | mg $NO_2$/L | - | - | 0.76[a] | 6.29[b] | 0.20[d] | Literature |
| $K_{NO2}$ | mg $NO_2$/L | - | 0.06 | - | - | - | Experimental |
| $K_{NO3}$ | mg $NO_2$/L | - | - | - | - | 0.20[d] | Literature |
| b | $d^{-1}$ | 0.15[c] | 0.05[c] | 0.05[c] | 0.05[f] | 0.40[d] | Literature |
| **Stoichiometric** | | | | | | | |
| Y | gCOD/ gN | 0.15[c] | 0.05[c] | 0.05[c] | 0.15[e] | | Literature |
| $Y_H$ | gCOD/gCOD | - | - | - | - | 0.6[d] | Literature |

$\mu$: Max. growth rate constant, $K_O$: Dissolved oxygen half-saturation constant, $K_{NH4}$: Ammonia half-saturation constant, $K_{NO2}$: Nitrite half-saturation constant, Y: Yield coefficient, b: Decay rate, a: (Yu et al., 2020), b: (Koch et al 2019), c: (Metcalf and Eddy 2003) d: (Hiatt and Grady, 2008), e: assumed equal to AOB (Roots et al. 2019), f: equal to NOB (Mehrani et al. 2021)

338 **Table 4.** Summarized information on the model efficiency during the calibration and validation periods

| Variable | Calibration phase | | | | Validation phase | | | | |
|---|---|---|---|---|---|---|---|---|---|
| | Trials | $R^2$ | RMSE | MAE | Trials | $R^2$ | RMSE | MAE | $J^2$ |
| $NH_4^+$-N | | 0.90 | 2.30 | 2.42 | | 0.87 | 2.58 | 3.11 | 1.25 |
| $NO_3^-$N | T 1 | 0.90 | 2.38 | 2.95 | T 2 | 0.86 | 2.72 | 3.25 | 1.30 |
| $NO_2^-$N | | 0.86 | 2.47 | 3.48 | | 0.81 | 3.44 | 3.67 | 1.93 |
| $NH_4^+$-N | | - | - | - | | - | - | - | - |
| $NO_3^-$N | T 3 | 0.90 | 2.32 | 2.62 | T 4 | 0.84 | 3.09 | 3.95 | 1.77 |
| $NO_2^-$N | | 0.88 | 2.56 | 2.69 | | 0.80 | 3.58 | 4.32 | 1.95 |

339

340 **3.4. Contribution of accompanying processes in N conversion**

341 Figure 7 shows the N conversion pathways in trial T1 with $NH_4^+$-N substrate. The relative
342 contributions of some bacteria groups were significantly shifted during the trial. The canonical
343 NOB1 and comammox bacteria continuously reduced their abundances - from 43 to 21% (NOB1)
344 and from 5% to 1% (comammox). The contribution of NOB2 was negligible (<0.1%). The AOB
345 increased their contribution from 38% at the beginning to 50% at the end of the trial. The
346 contribution of denitrifying heterotrophs, mediating two steps of denitrification, increased from
347 the initial 12.5% to 28% at the end of the trial.

348

349 Figure 8 shows the N conversion pathways in trial T3 with $NO_2^-$N substrate. The contribution of
350 NOB1 was substantially decreased from 79% to 7%, while the NOB2 contribution had an
351 increasing trend (4% to 89%) in the course of the trial. The comammox bacteria and denitrifying
352 heterotrophs decreased their contributions, respectively, from 4% to <1% and from 16% to 3%.

353

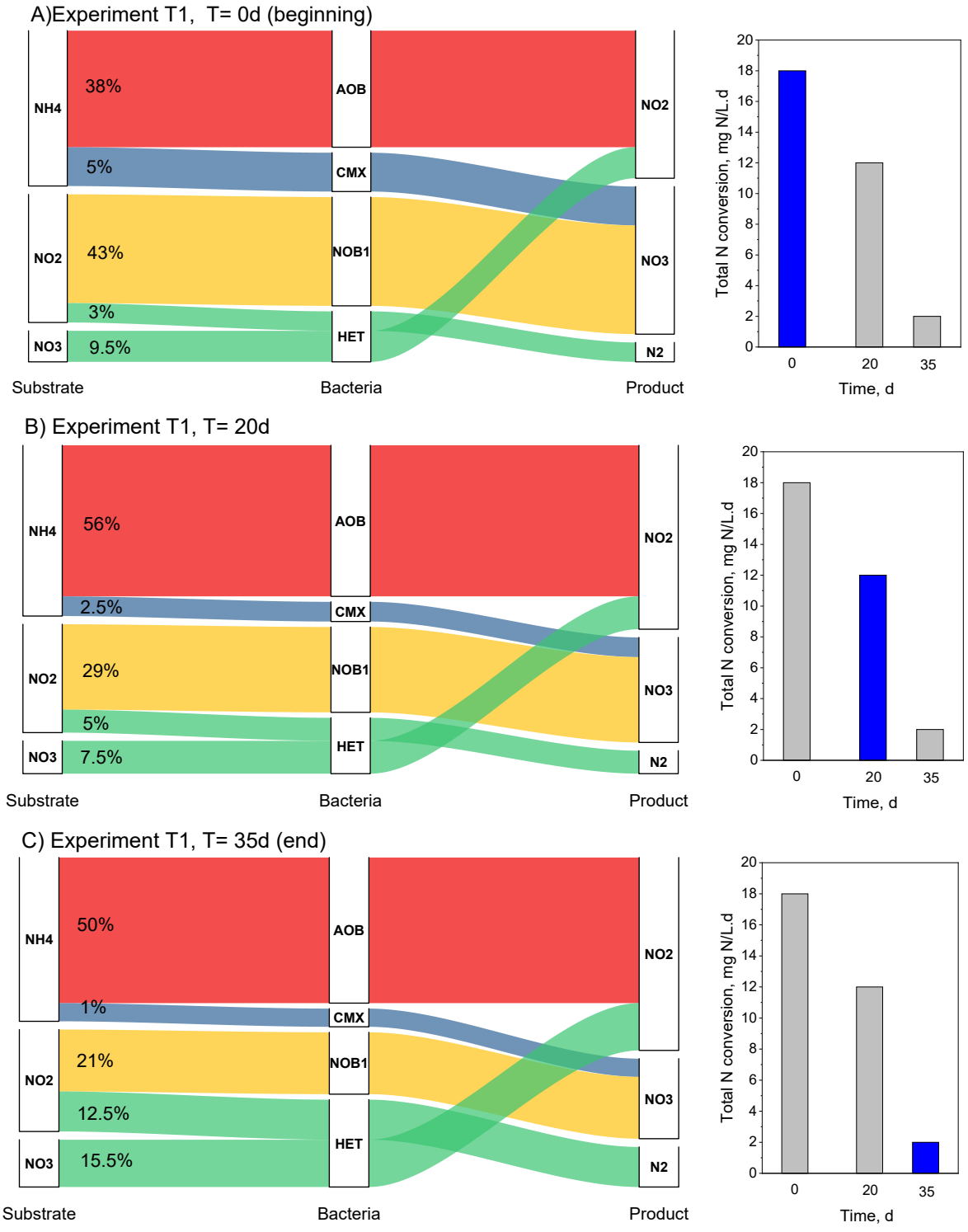


**Figure 7.** Sankey diagram showing the N conversion pathways in trial T1 (% represent the shares in the total conversion rate (mg N/L·d): A) 0 d, B) 20 d, C) 35 d

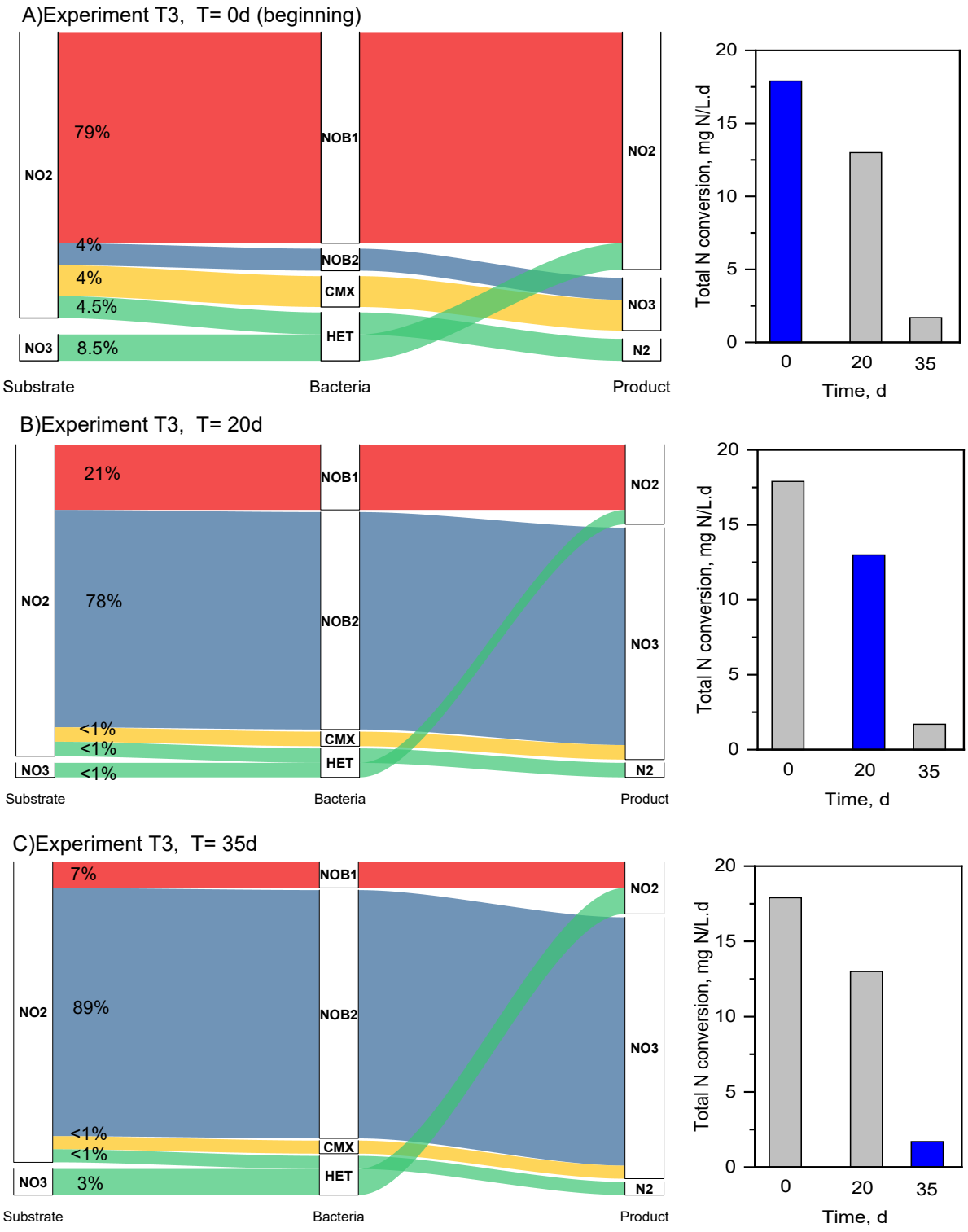


**Figure 8.** Conversion pathways of the N species for trial T3 (% represent the shares in the absolute total N conversions (mg N/L·d): A) 0 d, B) 20 d, C) 35 d

## 4. DISCUSSION

### 4.1. Factors influencing the competition between *Nitrospira* and *Nitrobacter*

In the present study, it has been confirmed that the NOB competition is predominantly impacted by substrate ($NO_2^-$N) concentrations, rather than temperature. Blackburne et al. (2007) attributed the dominance of *Nitrospira* over *Nitrobacter* under low $NH_4^+$-N and $NO_2^-$N concentrations to much lower inhibition thresholds of free ammonia (FA) and free nitrous acid (FNA). These thresholds were respectively 0.04–0.08 mg $NH_3$-N/L and 0.03 mg $HNO_2$-N/L for *Nitrospira*, and 10 mg $NH_3$-N/L and 0.2–0.4 mg $HNO_2$-N/L for *Nitrobacter*.

It has been shown in several studies (Huang et al., 2010; Nogueira and Melo, 2006; Park et al., 2017) that *Nitrobacter* was the dominating NOB at higher $NO_2^-$-N concentrations (> 80 mg N/L), whereas *Nitrospira* thrived better under lower $NO_2^-$-N conditions. Moreover, Nogueira and Melo (2006) observed that the dominance of *Nitrobacter* was not reverted after decreasing the $NO_2^-$-N concentration to the original (low) level. The authors provided two possible explanations for that observation, including inhibition of *Nitrospira* by high densities of *Nitrobacter* or not sufficient experimental period.

The DO concentration is another important operational factor that influences *Nitrospira* abundance in WWTPs ( Ushiki et al., 2017; Chang et al., 2019). Park et al. (2017) attributed a strong enrichment of *Nitrospira* (at the expense of *Nitrobacter*) in a DO- and $NO_2^-$-N -limited SBR to the lower affinity constants of *Nitrospira* for both substrates (see Table S5). (Liu and Wang, 2013) found that in addition to low DO concentrations (0.2-0.4 mg $O_2$/L), extending the SRT from 10 d to 40 d resulted in the dominance of *Nitrospira* over *Nitrobacter*.

Li et al., (2021) found that the SRT of 10 d and shorter aeration times (1.5 h) allowed to completely wash out NOB from the system. Gradually prolonged aeration times (3-3.5 h), applied subsequently, did not result in enriching NOB. Both *Nitrospira* and *Nitrobacter* abundances remained stable, but at a low level, which resulted in maintaining long-term $NO_2^-$-N accumulation in a wide temperature range (18-29 C).

*Nitrospira* may be better adapted to slightly higher pH (8–8.3 vs. 7.6–8.2) and temperatures (29–30 °C vs. 24–25 °C) in addition to low $NO_2^-$-N and DO concentrations. Sun et al., (2022) investigated the coexistence of *Nitrobacter* and *Nitrospira* at various pH (6.0-8.5). The optimum pH of 7.0 was found in terms of the maximum specific growth rate (μ) and substrate affinity ($K_{NO2}$) for $NO_2^-$-N oxidation, which also correlated with the highest absolute abundances of the functional genes of *Nitrobacter* (nxrA) and *Nitrospira* (nxrB).

Ushiki et al. (2017) hypothesized that *Nitrospira* had other characteristics to compete with *Nitrobacter* and other NOB in nitrite-limited environments. *Nitrobacter* has a cytoplasmic nitrite oxidoreductase (nxrA) that is responsible for the reverse transport of $NO_2^-$-N and $NO_3^-$-N through the inner membrane. On the contrary, *Nitrospira* encodes for periplasmic nxrB, which catalyses nitratation. The periplasmic oxidation is advantageous since it generates a larger specific proton motive force and avoids the transmembrane exchange of $NO_2^-$-N and $NO_3^-$-N (Pester et al., 2014).

Table S5 shows a literature review of the kinetic and stoichiometric parameters for *Nitrospira* and *Nitrobacter*. The ranges of $\mu$ for r-strategist *Nitrobacter* and K-strategist *Nitrospira* are 0.31-1.28 $d^{-1}$ and 0.15-0.93 $d^{-1}$, respectively. In the present study, the estimated $\mu$ for *Nitrobacter* (0.6

$d^{-1}$) was three times higher than *Nitrospira* (0.21 $d^{-1}$). In addition, the experimentally obtained Ko of 0.13 $mgO_2/L$ for NOB1 (*Nitrospira)* is slightly lower than the overall ranges in Table S6 ($K_{O,Nitrobacter}$= 0.17-4.32 $mgO_2/L$, $K_{O,Nitrospira}$= 0.33-1.35 $mgO_2/L$), while the optimized Ko of 0.45 $mgO_2/L$ for NOB2 is in the lower range (0.45-1.35 $mgO_2/L$) reported by Yu et al. (2020). It should be noted, however, that in the literature (O'Shaughnessy, 2016), the $K_O$ values for *Nitrospira* and other NOB genera were as low as 0.04 $d^{-1}$.

### 4.2. Role of comammox-*Nitrospira* in the systems fed with different N substrates

Maddela et al. (2021) noted that comammox bacteria have several competitive advantages over coexisting canonical nitrifiers, including the capability of thriving at low DO levels and a high substrate affinity. The high $NH_4^+$-N affinity of pure cultured comammox bacteria (*N. inopinata*) is indicated by extremely low half-saturation constants, which are 4- to 2500-fold lower than the values reported for AOB. Comammox bacteria also show a lower $NO_2^-$-N affinity than canonical NOB. Moreover, the abundances of comammox bacteria (*N. inopinata*) showed significant positive correlations with canonical NOB rather than AOB, which may suggest that comammox bacteria more actively mediate $NO_2^-$-N oxidation rather than $NH_4^+$-N oxidation. The authors concluded that switches between the modes of $NH_4^+$-N and $NO_2^-$-N oxidation in comammox bacteria remain unknown, and it is difficult to identify the environmental and operational factors determining the preferred nitrogen source.

The simulation results of the present study, strongly support the hypothesis that comammox bacteria can grow on $NO_2^-$-N. Following the discovery of comammox, it was thought that comammox-*Nitrospira*, do not possess this ability (Koch et al., 2019). Based on the findings of a previous investigation by Kits et al. (2017), this was explained by an extremely low $NO_2^-$-N

affinity. In comparison with canonical *Nitrospira*, *N. inopinata* (comammox bacteria) had a 50-fold lower $NO_2^-$-N affinity (Kits et al., 2017). In a recent study, Shao and Wu (2021) found that the $NO_2^-$-N affinities were variable among the comammox species. Under $NH_4^+$-N limiting conditions, some authors did not exclude the possibility of comammox bacteria using $NO_2^-$-N as electron donors (Kits et al., 2017; Palomo et al., 2018; Roots et al., 2019).

There is no consensus in the literature if $NO_2^-$-N is released outside of the cells during the comammox process. Kits et al. (2017) observed that comammox *Nitrospira* could produce $NO_2^-$-N as an extracellular transit product during complete nitrification. Transient $NO_2^-$-N accumulation produced by *N. inopinata* (comammox *Nitrospira*) during nitritation was reported by Ren et al. (2020). In contrast, Wu et al. (2020) found that comammox *Nitrospira* consumed $NH_4^+$-N and produced $NO_3^-$-N at the ratio of nearly 1:1 without any $NO_2^-$-N accumulation.

### 4.3. Further developments of two-NOB models describing the competition with other NOB groups

The model developed in the present study may be used to describe a competition of *Nitrospira* with NOB genera other than *Nitrobacter*. In particular, *Ca. Nitrotoga* has been detected as the main NOB genus, either alone or together with *Nitrospira*, in different full-scale WWTPs worldwide (Lücker et al., 2015; Saunders et al., 2016; Chen et al. 2020), and many pilot-scale systems (Figdore et al., 2018; Jiang et al., 2018; Persson et al., 2017; Wu et al., 2018; Zheng et al., 2019b). *Ca. Nitroto*a can oxidize $NO_2^-$-N at temperatures ranging from 4 to 28°C (Lantz et al., 2021), its optimum temperature (22-23°C) is lower compared to other NOB genera (Zheng et al., 2020; Ishii et al., 2020). Nowka et al. (2015) observed that *Ca. Nitrotoga* outcompeted *Nitrospira* and *Nitrobacter* during a long-term cultivation at 5 and 10°C. Liu et al. (2021)

calculated a very low temperature correction factor of 1.042 in the temperature range of 4-22 °C for NOB dominated by *Ca. Nitrotoga.* Speick et al. (2021) concluded that the adaptation of *Ca. Nitrotoga* to low temperatures may be beneficial for the recovery of nitratation during cold seasons.

$K_O$ for *Ca. Nitrotoga* has been determined by Zheng et al. (2020) as 0.59 ± 0.11 mg $O_2$/L. This value is slightly higher than Ko for *Nitrospira,* and much lower than *Nitrobacter* (see Table 5). Both *Nitrospira* and *Ca. Nitrotoga* resisted at intermittent aeration in a PN/A system (Gustavsson, 2020), whereas in another study, *Ca. Nitrotoga* was shown to have a lower DO affinity than *Nitrospira* (Zheng et al. 2020). Qian et al. (2021) found in a partial nitritation/anammox (PN/A) system that increasing the DO concentration from 0.4 to 1.8 mg$O_2$/L led to an increased abundance of *Ca. Nitrotoga* over *Nitrospira*. On the contrary, Jiang et al. (2018) found that a high DO of 2–2.5 mg$O_2$/L was sufficient for the washout of both *Nitrospira* and *Ca. Nitrotoga* in a PN/A system.

Higher substrate concentrations may be beneficial to *Nitrotoga* (Nowka et al. 2015). Kinnunen et al. (2017) discovered that at a $NO_2^-$-N concentration of 1 mg N/L, *Ca. Nitrotoga* outcompeted *Nitrospira* in a biofilm community, but *Nitrospira* dominated at a tenfold lower substrate concentration. $K_{NO2}$ for *Ca. Nitrotoga* was reported in a wide range of 0.345-1.68 mg N/L (Zheng et al., 2020; Kitzinger et al. 2018; Ishii et al. 2017; Wegen et al. 2019; Nowka et al. 2015). Ca. *Nitrotoga* was also shown to be much more resistant to free ammonia (FA) and free nitrous acid (FNA) exposure than *Nitrobacter* and *Nitrospira* (Li et al. 2020, Zheng et al., 2021).

The pH preference of *Ca. Nitrotoga* is neutral to slightly alkaline range as typical for nearly all NOB (Spieck et al., 2021). The optimum pH for *Ca. Nitrotoga* has been determined in a wide range as 7.1 – 7.6 (Kitzinger et al., 2018), 7.5 (Zheng et a., 2020), 8.3 (Ishii et al., 2020).

### 4.4. Interactions of nitrifiers and heterotrophs in N removal systems fed with inorganic carbon

In the present study, the strategy of progressive SRT reduction and the lack of organic carbon in the feed resulted in re-arrangements within the heterotrophic bacteria subpopulation (Table S2). Bacteria belonging to the order *Saprospiraceae* and genera *Caldilinea, Curvibacter*, *Dokdonella*, *Holophaga, Tetrasphaera* constituted predominant components in the inoculum biomass. However, during all the trials, those bacteria were systematically outcompeted by members of *Acidovorax*, *Hydrogenophaga*, *Comamonas*, *Pseudomonas*, *Simplicispira,* and *Thermomonas*.

Based on the reported characteristics of the identified heterotrophs, there are three possible mechanisms of the surveillance and competitiveness of those bacteria in comparison with other heterotrophs under extremely short SRTs and inorganic feeding medium: (i) heterotrophic denitrification with soluble microbial products (SMP) and extracellular polymeric substances (EPS), generated by AOB and NOB (Nogueira et al. 2005; Sepehri and Sarrafzadeh 2019), (ii) heterotrophic nitrification (Chen et al. 2012), (iii) predation of heterotrophs on autotrophic bacteria (Dolinšek et al. 2013).

In particular, during the trials with $NH_4$-N as a sole N source, a wider range and more equally represented heterotrophic bacteria groups have been detected during the final stages. Similar to the present study, a noticeable occurrence of the *Acidovorax* and *Pseudomonas* representatives in

511 the reactor fed with an inorganic medium was observed by Keluskar et al. (2013). The growth of
512 those heterotrophs was supported by organic compounds, such as pyruvate, excreted by AOB
513 (*Nitrosomonas*). An additional metabolic pathway enabling the survival of specific heterotrophs
514 (*Hydrogenophaga*) in the systems operated under the limited carbon availability is
515 hydrogenotrophic denitrification with the utilization of hydrogen in the absence of organic
516 compounds. Furthermore, representatives of *Rhodococcus* have been characterized as bacteria
517 which are capable of performing simultaneous heterotrophic nitrification and aerobic
518 denitrification (Chen et, al 2012).
519
520 In the present study, in the trials with $NO_2$-N as a sole N source, members of the *Comamonas*
521 genera outcompeted other heterotrophs, and their relative abundances exceeded 50% in both trails
522 (at 12 and 20°C). Representatives of the *Comamonas* are well known denitrifying heterotrophs,
523 which are capable of utilizing a wide range of organic compounds, such as amino acids,
524 carboxylic acids, steroids and aromatic compounds (Wu et al., 2018), thus due to wide metabolic
525 properties were capable to develop substrate dependencies with *Nitrobacter* NOB.
526
527 Predation is another factor affecting the occurrence of specific heterotrophs and their interaction
528 with the nitrifiers (Dolinšek et al. 2013). Daims et al. (2016) showed that abundances of
529 *Nitrospira* were dramatically reduced due to the predation by *B. bacteriovorus*. In the present
530 study, during the trials with $NH_4$-N, predator bacteria belonging to the *Bdellovibrio* genus were
531 detected in the abundances > 3%. On the other hand, lower abundances of these bacteria were
532 found during the trials with $NO_2$-N, when *Nitrobacter* was predominant. This finding suggests
533 that predation may indeed reflect a selective pressure on specific NOB.
534

## 5. CONCLUSIONS

- A two-step nitrification model was extended with different NOB groups (competing r strategists vs. K strategists) to increase the prediction accuracy of modeling nitrifying systems under diverse $NO_2^-$-N availabilities in the substrate.
- In addition to the standard prediction parameters (N species and biomass concentrations), microbiological indicators such as the relative abundance of comammox and the ratio of nitrifiers to heterotrophs, are useful target variables for calibration of mechanistic models as they revealed the dominant conversion pathways in the studied systems.
- A combination of microbiological analyses and modeling simulation results confirmed that comammox bacteria can grow on $NO_2^-$-N as a sole N substrate.
- In contrast to canonical nitrifiers, comammox played a minor role in the study system. However, the impact of these bacteria needs to be further explored by modeling systems containing a higher abundance of *Nitrospira*.
- Even though comammox played a minor role in the studied system compared to the canonical nitrifiers, the impact of these bacteria should further be explored by modeling systems containing a higher abundances of *Nitrospira*.

## ACKNOWLEDGMENTS

This study was supported by the Polish National Science Center under project no. UMO-2017/27/B/NZ9/01039.

## REFERENCES


Al-Hazmi HE, Lu X, Majtacz J, Kowal P, Xie L, Makinia J. Optimization of the Aeration Strategies in a Deammonification Sequencing Batch Reactor for Efficient Nitrogen Removal and Mitigation of $N_2O$ Production. Environmental Science & Technology 2021; 55: 1218-1230.

Blackburne R, Vadivelu VM, Yuan Z, Keller J. Kinetic characterisation of an enriched Nitrospira culture with comparison to Nitrobacter. Water Research 2007; 41: 3033-3042.

Cao J, Zhang T, Wu Y, Sun Y, Zhang Y, Huang B, et al. Correlations of nitrogen removal and core functional genera in full-scale wastewater treatment plants: Influences of different treatment processes and influent characteristics. Bioresource Technology 2020; 297: 122455.

Cao Y, van Loosdrecht MCM, Daigger GT. Mainstream partial nitritation–anammox in municipal wastewater treatment: status, bottlenecks, and further studies. Applied Microbiology and Biotechnology 2017; 101: 1365-1383.

Chang M, Wang Y, Pan Y, Zhang K, Lyu L, Wang M, et al. Nitrogen removal from wastewater via simultaneous nitrification and denitrification using a biological folded non-aerated filter. Bioresource Technology 2019; 289: 121696.

Chen P, Li J, Li QX, Wang Y, Li S, Ren T, et al. Simultaneous heterotrophic nitrification and aerobic denitrification by bacterium Rhodococcus sp. CPZ24. Bioresource Technology 2012; 116: 266-270.

Chen H, Wang M, Chang S. Disentangling Community Structure of Ecological System in Activated Sludge: Core Communities, Functionality, and Functional Redundancy. Microbial Ecology 2020; 80: 296-308.

Daims H, Lücker S, Wagner M. A New Perspective on Microbes Formerly Known as Nitrite-Oxidizing Bacteria. Trends in Microbiology 2016; 24: 699-712.

582 Daims H, Lebedeva EV, Pjevac P, Han P, Herbold C, Albertsen M, et al. Complete nitrification by
583 Nitrospira bacteria. Nature 2015; 528: 504.
584 Dolinšek J, Lagkouvardos I, Wanek W, Wagner M, Daims H. Interactions of Nitrifying Bacteria
585 and Heterotrophs: Identification of a Micavibrio-Like Putative Predator of Nitrospira spp.
586 Applied and Environmental Microbiology 2013; 79: 2027-2037.
587 Duan H, Ye L, Wang Q, Zheng M, Lu X, Wang Z, et al. Nitrite oxidizing bacteria (NOB) contained
588 in influent deteriorate mainstream NOB suppression by sidestream inactivation. Water
589 Research 2019; 162: 331-338.
590 Feng S, Tan CH, Constancias F, Kohli GS, Cohen Y, Rice SA. Predation by Bdellovibrio
591 bacteriovorus significantly reduces viability and alters the microbial community
592 composition of activated sludge flocs and granules. FEMS Microbiology Ecology 2017; 93:
593 20-28.
594 Figdore BA, Stensel HD, Winkler M-KH. Comparison of different aerobic granular sludge types
595 for activated sludge nitrification bioaugmentation potential. Bioresource Technology 2018;
596 251: 189-196.
597 Gustavsson DJI, Suarez C, Wilén B-M, Hermansson M, Persson F. Long-term stability of partial
598 nitritation-anammox for treatment of municipal wastewater in a moving bed biofilm reactor
599 pilot system. Science of The Total Environment 2020; 714: 136342.
600 Hauduc H, Neumann MB, Muschalla D, Gamerith V, Gillot S, Vanrolleghem PA. Efficiency
601 criteria for environmental model quality assessment: A review and its application to
602 wastewater treatment. Environmental Modelling & Software 2015; 68: 196-204.
603 Henze MG, W., Mino, T., van Loosdrecht, M.C.M. Activated sludge models ASM1, ASM2,
604 ASM2d and ASM3. London, UK: IWA Publishing, 2000.

605 Hiatt WC, Grady CPL. An Updated Process Model for Carbon Oxidation, Nitrification, and
606 Denitrification. Water Environment Research 2008; 80: 2145-2156.
607 Huang Z, Gedalanga PB, Asvapathanagul P, Olson BH. Influence of physicochemical and
608 operational parameters on Nitrobacter and Nitrospira communities in an aerobic activated
609 sludge bioreactor. Water Research 2010; 44: 4351-4358.
610 Ishii K, Fujitani H, Sekiguchi Y, Tsuneda S. Physiological and genomic characterization of a new
611 'Candidatus Nitrotoga' isolate. Environmental Microbiology 2020; 22: 2365-2382.
612 Jiang H, Liu G-h, Ma Y, Xu X, Chen J, Yang Y, et al. A pilot-scale study on start-up and stable
613 operation of mainstream partial nitrification-anammox biofilter process based on online
614 pH-DO linkage control. Chemical Engineering Journal 2018; 350: 1035-1042.
615 Keene NA, Reusser SR, Scarborough MJ, Grooms AL, Seib M, Santo Domingo J, et al. Pilot plant
616 demonstration of stable and efficient high rate biological nutrient removal with low
617 dissolved oxygen conditions. Water Research 2017; 121: 72-85.
618 Keluskar R, Nerurkar A, Desai A. Mutualism between autotrophic ammonia-oxidizing bacteria
619 (AOB) and heterotrophs present in an ammonia-oxidizing colony. Archives of
620 Microbiology 2013; 195: 737-747.
621 Kent TR, Sun Y, An Z, Bott CB, Wang Z-W. Mechanistic understanding of the NOB suppression
622 by free ammonia inhibition in continuous flow aerobic granulation bioreactors.
623 Environment International 2019; 131: 105005.
624 Kinnunen M, Gülay A, Albrechtsen H-J, Dechesne A, Smets BF. Nitrotoga is selected over
625 Nitrospira in newly assembled biofilm communities from a tap water source community at
626 increased nitrite loading. Environmental Microbiology 2017; 19: 2785-2793.
627 Kits KD, Sedlacek CJ, Lebedeva EV, Han P, Bulaev A, Pjevac P, et al. Kinetic analysis of a
628 complete nitrifier reveals an oligotrophic lifestyle. Nature 2017; 549: 269-272.

629 Koch H, van Kessel MAHJ, Lücker S. Complete nitrification: insights into the ecophysiology of
630 comammox Nitrospira. Applied Microbiology and Biotechnology 2019; 103: 177-189.
631 Laanbroek HJ, Bodelier PLE, Gerards S. Oxygen consumption kinetics of Nitrosomonas europaea
632 and Nitrobacter hamburgensis grown in mixed continuous cultures at different oxygen
633 concentrations. Archives of Microbiology 1994; 161: 156-162.
634 Lantz MA, Boddicker AM, Kain MP, Berg OMC, Wham CD, Mosier AC. Physiology of the
635 Nitrite-Oxidizing Bacterium Candidatus Nitrotoga sp. CP45 Enriched From a Colorado
636 River. Frontiers in microbiology 2021; 12: 709371-709371.
637 Lawson CE, Lücker S. Complete ammonia oxidation: an important control on nitrification in
638 engineered ecosystems? Current Opinion in Biotechnology 2018; 50: 158-165.
639 Li S, Duan H, Zhang Y, Huang X, Yuan Z, Liu Y, et al. Adaptation of nitrifying community in
640 activated sludge to free ammonia inhibition and inactivation. Science of The Total
641 Environment 2020; 728: 138713.
642 Li S, Li J, Yang S, Zhang Q, Li X, Zhang L, et al. Rapid achieving partial nitrification in domestic
643 wastewater: Controlling aeration time to selectively enrich ammonium oxidizing bacteria
644 (AOB) after simultaneously eliminating AOB and nitrite oxidizing bacteria (NOB).
645 Bioresource Technology 2021; 328: 124810.
646 Liu G, Wang J. Long-Term Low DO Enriches and Shifts Nitrifier Community in Activated Sludge.
647 Environmental Science & Technology 2013; 47: 5109-5117.
648 Liu H, Zhu L, Tian X, Yin Y. Seasonal variation of bacterial community in biological aerated filter
649 for ammonia removal in drinking water treatment. Water Research 2017; 123: 668-677.
650 Liu X, Huang M, Bao S, Tang W, Fang T. Nitrate removal from low carbon-to-nitrogen ratio
651 wastewater by combining iron-based chemical reduction and autotrophic denitrification.
652 Bioresource Technology 2020; 301: 122731.

653 Liu Y, Li S, Ni G, Duan H, Huang X, Yuan Z, et al. Temperature Variations Shape Niche
654 Occupation of Nitrotoga-like Bacteria in Activated Sludge. ACS ES&T Water 2021; 1:
655 167-174.
656 Lücker S, Schwarz J, Gruber-Dorninger C, Spieck E, Wagner M, Daims H. Nitrotoga-like bacteria
657 are previously unrecognized key nitrite oxidizers in full-scale wastewater treatment plants.
658 The ISME Journal 2015; 9: 708-720.
659 Ma Y, Domingo-Félez C, Plósz BG, Smets BF. Intermittent Aeration Suppresses Nitrite-Oxidizing
660 Bacteria in Membrane-Aerated Biofilms: A Model-Based Explanation. Environmental
661 Science & Technology 2017; 51: 6146-6155.
662 Maddela NR, Gan Z, Meng Y, Fan F, Meng F. Occurrence and Roles of Comammox Bacteria in
663 Water and Wastewater Treatment Systems: A Critical Review. Engineering 2021; 0-
664 Mehrani M-J, Lu X, Sobotka D, Kowal P, Makinia J. Incorporation of the complete ammonia
665 oxidation (comammox) process for nitrification modeling in activated sludge systems.
666 Journal of Environmental Management 2021; 297: 113223.
667 Mehrani M-J, Sobotka D, Kowal P, Ciesielski S, Makinia J. The occurrence and role of Nitrospira
668 in nitrogen removal systems. Bioresource Technology 2020; 303: 122936.
669 Mehrani M-J, Sobotka D, Kowal P, Guo J, Mąkinia J. New insights into modeling two-step
670 nitrification in activated sludge systems – the effects of initial biomass concentrations,
671 comammox and heterotrophic activities. Science of the Total Environment 2022, 157628.
672 Metcalf and Eddy, Inc., Wastewater Engineering: Treatment and Resource Recovery, 5th Edition.
673 McGraw-Hill , New York, United States, 2014.
674 Metcalf and Eddy, Inc., Wastewater Engineering : Treatment and Reuse, 4th Edition. McGraw-
675 Hill, New York, United States, 2003.

676 Metcalf and Eddy, Inc., Wastewater Engineering: Treatment, Disposal, and Reuse, 3rd Edition.
677 McGraw-Hill, New York, United States, 1990.
678 Nogueira R, Melo LF. Competition between Nitrospira spp. and Nitrobacter spp. in nitrite-
679 oxidizing bioreactors. Biotechnology and Bioengineering 2006; 95: 169-175.
680 Nogueira R, Elenter D, Brito A, Melo LF, Wagner M, Morgenroth E. Evaluating heterotrophic
681 growth in a nitrifying biofilm reactor using fluorescence in situ hybridization and
682 mathematical modeling. Water Science and Technology 2005; 52: 135-141.
683 Nowka B, Daims H, Spieck E. Comparison of Oxidation Kinetics of Nitrite-Oxidizing Bacteria:
684 Nitrite Availability as a Key Factor in Niche Differentiation. Applied and Environmental
685 Microbiology 2015; 81: 745.
686 O'Shaughnessy M. Mainstream Deammonification (WERF Report INFR6R11). Water
687 Environment Research Foundation, 2016, Alexandria, VA (USA).
688 Palomo A, Pedersen AG, Fowler SJ, Dechesne A, Sicheritz-Pontén T, Smets BF. Comparative
689 genomics sheds light on niche differentiation and the evolutionary history of comammox
690 Nitrospira. Isme j 2018; 12: 1779-1793.
691 Park M-R, Park H, Chandran K. Molecular and Kinetic Characterization of Planktonic Nitrospira
692 spp. Selectively Enriched from Activated Sludge. Environmental Science & Technology
693 2017; 51: 2720-2728.
694 Pérez J, Lotti T, Kleerebezem R, Picioreanu C, van Loosdrecht MCM. Outcompeting nitrite-
695 oxidizing bacteria in single-stage nitrogen removal in sewage treatment plants: A model-
696 based study. Water Research 2014; 66: 208-218.
697 Persson F, Suarez C, Hermansson M, Plaza E, Sultana R, Wilén B-M. Community structure of
698 partial nitritation-anammox biofilms at decreasing substrate concentrations and low
699 temperature. Microbial Biotechnology 2017; 10: 761-772.

Qian F, Huang Z, Liu Y, Grace OOw, Wang J, Shi G. Conversion of full nitritation to partial nitritation/anammox in a continuous granular reactor for low-strength ammonium wastewater treatment at 20 °C. Biodegradation 2021; 32: 87-98.

Regmi P, Miller MW, Holgate B, Bunce R, Park H, Chandran K, et al. Control of aeration, aerobic SRT and COD input for mainstream nitritation/denitritation. Water Research 2014; 57: 162-171.

Roots P, Wang Y, Rosenthal AF, Griffin JS, Sabba F, Petrovich M, et al. Comammox Nitrospira are the dominant ammonia oxidizers in a mainstream low dissolved oxygen nitrification reactor. Water Research 2019; 157: 396-405.

Sakoula D, Koch H, Frank J, Jetten MSM, van Kessel MAHJ, Lücker S. Enrichment and physiological characterization of a novel comammox Nitrospira indicates ammonium inhibition of complete nitrification. The ISME Journal 2021; 15: 1010-1024.

Saunders AM, Albertsen M, Vollertsen J, Nielsen PH. The activated sludge ecosystem contains a core community of abundant organisms. The ISME Journal 2016; 10: 11-20.

Sepehri A, Sarrafzadeh M-H. Activity enhancement of ammonia-oxidizing bacteria and nitrite-oxidizing bacteria in activated sludge process: metabolite reduction and CO2 mitigation intensification process. Applied Water Science 2019; 9: 131.

Shao Y-H, Wu J-H. Comammox Nitrospira Species Dominate in an Efficient Partial Nitrification–Anammox Bioreactor for Treating Ammonium at Low Loadings. Environmental Science & Technology 2021; 55: 2087-2098.

Spieck E, Wegen S, Keuter S. Relevance of Candidatus Nitrotoga for nitrite oxidation in technical nitrogen removal systems. Applied Microbiology and Biotechnology 2021; 105: 7123-7139.

722 Sun H, Zhang H, Zhang F, Yang H, Lu J, Ge S, et al. Response of substrate kinetics and biological
723 mechanisms to various pH constrains for cultured Nitrobacter and Nitrospira in nitrifying
724 bioreactor. Journal of Environmental Management 2022; 307: 114499.
725 Ushiki N, Jinno M, Fujitani H, Suenaga T, Terada A, Tsuneda S. Nitrite oxidation kinetics of two
726 Nitrospira strains: The quest for competition and ecological niche differentiation. Journal
727 of Bioscience and Bioengineering 2017; 123: 581-589.
728 Vadivelu VM, Yuan Z, Fux C, Keller J. Stoichiometric and kinetic characterisation of Nitrobacter
729 in mixed culture by decoupling the growth and energy generation processes. Biotechnology
730 and Bioengineering 2006; 94: 1176-1188.
731 van Kessel MAHJ, Speth DR, Albertsen M, Nielsen PH, Op den Camp HJM, Kartal B, et al.
732 Complete nitrification by a single microorganism. Nature 2015; 528: 555.
733 Wegen S, Nowka B, Spieck E. Low Temperature and Neutral pH Define "Candidatus Nitrotoga
734 sp." as a Competitive Nitrite Oxidizer in Coculture with Nitrospira defluvii. Appl Environ
735 Microbiol 2019; 85.
736 Winkler MKH, Boets P, Hahne B, Goethals P, Volcke EIP. Effect of the dilution rate on microbial
737 competition: r-strategist can win over k-strategist at low substrate concentration. PLOS
738 ONE 2017; 12: e0172785.
739 Wu L, Ning D, Zhang B, Li Y, Zhang P, Shan X, et al. Global diversity and biogeography of
740 bacterial communities in wastewater treatment plants. Nature Microbiology 2019; 4: 1183-
741 1195.
742 Wu L, Li Z, Zhao C, Liang D, Peng Y. A novel partial-denitrification strategy for post-anammox
743 to effectively remove nitrogen from landfill leachate. Science of The Total Environment
744 2018; 633: 745-751.

Yin Q, Sun Y, Li B, Feng Z, Wu G, The r/K selection theory and its application in biological wastewater treatment processes. Science of the Total Environment 2022; 824: 153836

Yu L, Chen S, Chen W, Wu J. Experimental investigation and mathematical modeling of the competition among the fast-growing "r-strategists" and the slow-growing "K-strategists" ammonium-oxidizing bacteria and nitrite-oxidizing bacteria in nitrification. Science of The Total Environment 2020; 702: 135049.

Zaborowska E, Lu X, Mąkinia J. Strategies for mitigating nitrous oxide production and decreasing the carbon footprint of a full-scale combined nitrogen and phosphorus removal activated sludge system. Water Research 2019; 162: 53-63.

Zheng M, Li S, Ni G, Xia J, Hu S, Yuan Z, et al. Critical Factors Facilitating Candidatus Nitrotoga To Be Prevalent Nitrite-Oxidizing Bacteria in Activated Sludge. Environmental Science & Technology 2020; 54: 15414-15423.

Zheng M, Li S, Dong Q, Huang X, Liu Y. Effect of blending landfill leachate with activated sludge on the domestic wastewater treatment process. Environmental Science: Water Research & Technology 2019a; 5: 268-276.

Zheng Z, Huang S, Bian W, Liang D, Wang X, Zhang K, et al. Enhanced nitrogen removal of the simultaneous partial nitrification, anammox and denitrification (SNAD) biofilm reactor for treating mainstream wastewater under low dissolved oxygen (DO) concentration. Bioresource Technology 2019b; 283: 213-220.

Zhu A, Guo J, Ni B-J, Wang S, Yang Q, Peng Y. A Novel Protocol for Model Calibration in Biological Wastewater Treatment. Scientific Reports 2015; 5: 8493.

# Supplementary Information

## *The coexistence and competition of canonical and comammox nitrite oxidizing bacteria in a nitrifying activated sludge system – experimental observations and simulation studies*

**Mohamad-Javad Mehrani [1], Przemyslaw Kowal[1], Dominika Sobotka[1], Martyna Godzieba[2], Slawomir Ciesielski [2], Jianhua Guo[3], Jacek Makinia[1*]**

[1] Faculty of Civil and Environmental Engineering, Gdansk University of Technology, Narutowicza Street 11/12, 80-233 Gdansk, Poland

[2] Department of Environmental Biotechnology, Department of Environmental Biotechnology, University of Warmia and Mazury in Olsztyn, Sloneczna 45G, 10-719 Olsztyn, Poland

[3]Australian Centre for Water and Environmental Biotechnology (ACWEB, formerly AWMC), The University of Queensland, St. Lucia, Queensland 4072, Australia

*Correspondence: Jacek Makinia (Email: jmakinia@pg.edu.pl, Tel: +48 58 347 19 54, Address: Gdansk University of Technology, ul. Narutowicza 11/12, 80-233, Gdansk, Poland)

## S1. Synthetic medium used for the long-term experiments and Influent substrate concentrations

**Table S1.** Characteristics of the synthetic medium ($NH_4$-N vs. $NO_2$-N substrate) used for the long-term washout experiments

| Substrate | Main elements | | Tracer solution* | |
|---|---|---|---|---|
| | Compound | Concentration mg/L | Compound | Concentration g/L |
| **$NH_4$-N** | $NH_4CL$ | 762 | $ZnSO_4 \cdot 7H_2O$ | 0.43 |
| | $KHCO_3$ | 1512 | $(NH_4)_6Mo_7O_{24} \cdot 4H_2O$ | 0.22 |
| | $CaCl_2$ | 141 | $CuSO_4 \cdot 5H_2O$ | 0.25 |
| | $KH_2PO_4$ | 50 | $MnCl_2 \cdot 4H_2O$ | 0.99 |
| | $MgSO_4$ | 58.6 | $CoCl_2 \cdot 6H_2O$ | 0.24 |
| | $FeSO_4 \cdot 7H_2O$ | 9.1 | $NaWO_4 \cdot 2H_2O$ | 0.005 |
| | EDTA | 6.3 | EDTA | 15 |
| | Tracer solution* | 1 | $NiCl_2 \cdot 6H_2O$ | 0.2 |
| | | | $NaSeO_4 \cdot 10H_2O$ | 0.2 |
| | | | $H_3BO_3$ | 0.014 |
| **$NO_2$-N** | $NO_2^-$ | 172 - 1470 | $ZnSO_4 \cdot 7H_2O$ | 0.43 |
| | $KHCO_3$ | 1512 | $(NH_4)_6Mo_7O_{24} \cdot 4H_2O$ | 0.22 |
| | $CaCl_2$ | 141 | $CuSO_4 \cdot 5H_2O$ | 0.25 |
| | $KH_2PO_4$ | 50 | $MnCl_2 \cdot 4H_2O$ | 0.99 |
| | $MgSO_4$ | 58.6 | $CoCl_2 \cdot 6H_2O$ | 0.24 |
| | $FeSO_4 \cdot 7H_2O$ | 9.1 | $NaWO_4 \cdot 2H_2O$ | 0.005 |
| | EDTA | 6.3 | EDTA | 15 |
| | Tracer solution* | 1 | $NiCl_2 \cdot 6H_2O$ | 0.2 |
| | | | $NaSeO_4 \cdot 10H_2O$ | 0.2 |
| | | | $H_3BO_3$ | 0.014 |

789

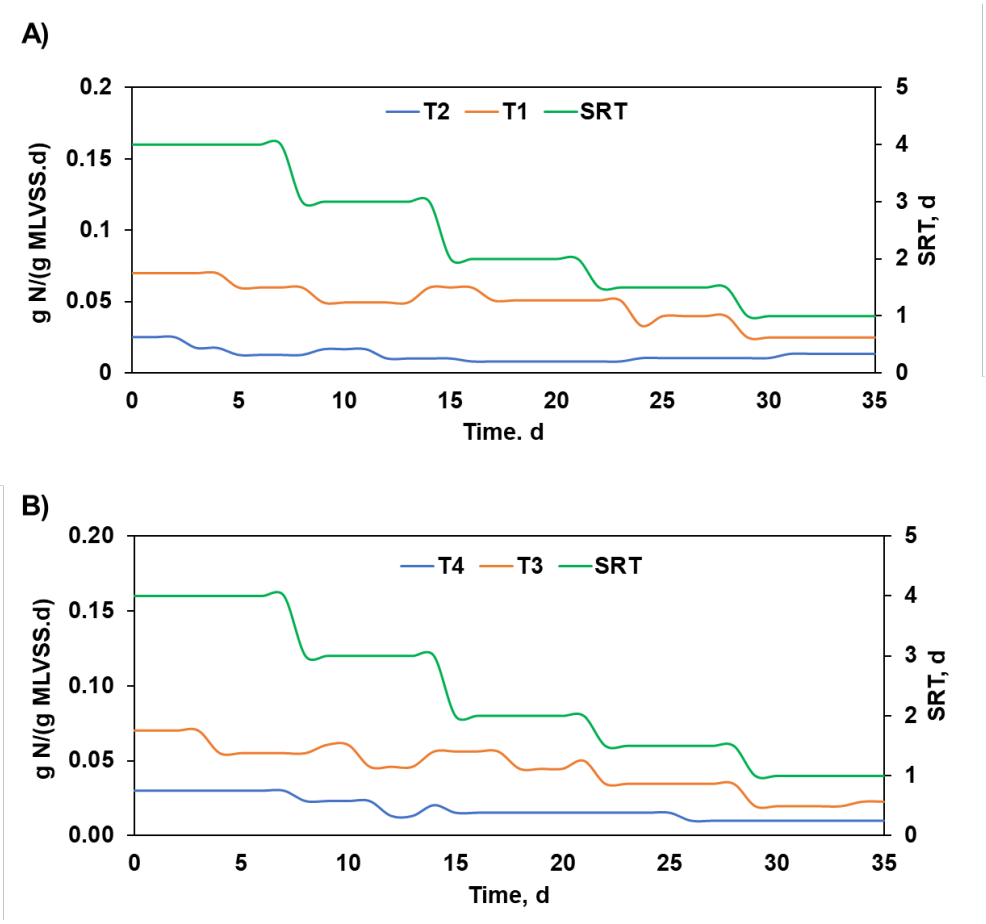


**Figure S1-** SRT and influent N loading rate for A) $NH_4^+$-N substrate experiments (T1, T2), and B) $NO_2^-$-N substrate experiments (T3, T4)

## S2. Microbiological analytical methods

### *S.2.1. DNA extraction*

Biomass samples for microbial analysis were collected from the SBRs three times: at the beginning (inoculum), during the middle phase (25th day), and at the of the experiment (35th day). The biomass samples from the initial experimental stages were transferred to the 50 ml Falcon type tubes for sedimentation and thickening. The biomass samples withdrawn during the terminal stages, were separated from the outflows from the experimental SBR by filtration trough through 0.22 μm pore size filters. Each sample was collected in duplicate. Both types of the samples (thickened sludge and biomass deposited on filters) were stored at −25°C prior to DNA extraction. The

803 extraction of the DNA from the biomass samples (100 mg of the thickened sludge or filter slices
804 with deposited biomass) was carried out using the FastDNA™ SPIN KIT (MP Biomedicals, USA)
805 following the manufacturer's manual. The DNA acquired from purification was subsequently used
806 for the Illumina Next Generation Sequencing protocol.
807
808 ***S.2.2. High-throughput 16S rDNA sequencing***
809 High-throughput Illumina sequencing targeting the V3-V4 region of the 16S rRNA gene was
810 performed with S-d-Bact-0341-b-S-17 and S-d-Bact-0785-a-A-21 primers (Klindworth et al., 2012)
811 and NEBNext®High-Fidelity 2X PCR Master Mix (Bio Labs inc., USA) following the
812 manufacturer's manual. The sequencing reactions were carried out with MiSeq sequencer (Illumina,
813 USA) by applying the paired-end technology, 2×250 nt with MiSeq Reagent Kit V2 following the
814 manufacturer's protocols. The obtained raw DNA sequence reads were subjected to quality control
815 (QC) using the tools available at Useqalaxy server (usegalaxy.org). Paired-end reads were initially
816 combined with the fastq-join algorithm. The reads were subsequently trimmed and filtered in terms
817 of the length (≥ 400 bp) and quality (Phred score ≥ 20) with Filter FASTQ algorithm. The reads
818 quality at each QC step was validated with FastQC software
819 (www.bioinformatics.babraham.ac.uk/projects/fastqc).
820
821 Chimera presence was verified with a chimera check on-line tool powered by UCHIME
822 (http://pyro.cme.msu.edu). The classification of the reads on each taxonomical level was carried
823 out with the SILVA server (www.arb-silva.de) using the database release version 132 at the
824 similarity level of 90% and operational taxonomic units (OTUs) clustering at 97%. The output data
825 from the Usegalaxy server were saved into FASTA format and uploaded to the MetaGenome Rapid

826 Annotation Subsystems Technology (MG-RAST) (Meyer et al., 2008) to enable public access to
827 the files under the accession numbers ranging from mgm4899014.3 to mgm4899025.3.
828
829 ***S.2.3 Absolute quantification of the Comammox bacteria by qPCR***
830 Absolute quantification of the comammox amoA genes was performed with primers sets comaA-
831 244F & comaA-659R and comaB-244F & comaB-659R in order detect and enumerate comammox
832 *Nitrospira* clades A and B, respectively, in accordance with the protocol proposed by (Pjevac et
833 al., 2017). The real-time PCR reactions were performed on ABI 7500 real-time PCR thermocycler
834 (Applied Biosystems) in MicroAmpTM Optical 96-well reaction plates (Applied Biosystems).
835 Each sample was analysed in triplicate.
836

837 **Table S2.** Composition of the overall bacterial community and dynamics of the most abundant HET bacteria during
838 particular experimental trials. The relative abundances are presented in the form of the heatmap in accordance to the
839 presented pattern 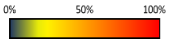


| Experimental series (day of the experiment) | $NO_2$-N only; 12°C | | | $NO_2$-N only; 20°C | | | $NH_4$-N only; 12°C | | | $NH_4$-N only; 20°C | | |
|---|---|---|---|---|---|---|---|---|---|---|---|---|
| | T1 | | | T2 | | | T3 | | | T4 | | |
| BLAST assignment (at >85% similarity) | 1 | 15 | 28 | 1 | 14 | 30 | 1 | 21 | 35 | 1 | 21 | 35 |
| uncultured member of Saprospiraceae (HET) | 7.1% | 3.7% | 0.1% | 7.6% | 3.4% | 0.0% | 4.16% | 1.52% | 0.43% | 7.26% | 0.08% | 0.69% |
| *Curvibacter (DEN)* | 7.5% | 1.9% | 0.1% | 3.7% | 0.9% | 0.0% | 0.0% | 0.2% | 0.0% | 0.2% | 0.2% | 0.1% |
| *Tetrasphaera (DPAO)* | 3.5% | 2.8% | 0.0% | 4.8% | 2.1% | 0.0% | 3.7% | 0.6% | 0.1% | 3.0% | 0.0% | 0.2% |
| *Candidatus* Saccharibacteria *(DEN)* | 1.8% | 1.3% | 0.0% | 1.0% | 0.5% | 0.1% | 5.5% | 1.8% | 0.5% | 4.5% | 1.3% | 0.3% |
| *Dokdonella (DEN)* | 4.5% | 3.6% | 0.5% | 1.9% | 3.3% | 0.1% | 1.5% | 1.3% | 1.0% | 2.3% | 0.7% | 4.9% |
| *Gemmatimonas (DPAO)* | 1.2% | 0.9% | 0.1% | 1.3% | 1.4% | 0.0% | 1.5% | 1.1% | 0.3% | 1.8% | 0.0% | 1.3% |
| *Holophaga (HET)* | 2.2% | 2.0% | 0.1% | 0.9% | 1.0% | 0.0% | 2.4% | 0.8% | 0.2% | 3.1% | 0.0% | 0.5% |
| *Thermomonas(DEN)* | 4.3% | 0.9% | 1.0% | 3.5% | 2.5% | 0.1% | 0.3% | 2.2% | 2.7% | 0.8% | 3.7% | 3.1% |
| *Candidatus* Microthrix *(DPAO)* | 2.4% | 0.8% | 0.1% | 3.0% | 1.8% | 0.0% | 2.5% | 0.5% | 0.1% | 1.4% | 0.0% | 0.1% |
| *Acidovorax (DEN)* | 4.7% | 7.9% | 2.7% | 8.0% | 16.2% | 1.1% | 1.6% | 11.3% | 12.6% | 1.4% | 2.7% | 3.2% |
| *Terrimonas (HET)* | 2.1% | 1.6% | 0.2% | 2.4% | 1.5% | 0.1% | 1.0% | 0.7% | 0.6% | 0.9% | 0.2% | 1.1% |
| *Caldilinea (HET/DEN)* | 2.4% | 2.5% | 0.1% | 1.7% | 2.5% | 0.1% | 5.8% | 1.6% | 0.4% | 4.8% | 0.2% | 1.0% |
| *Pelomonas (DEN)* | 1.0% | 6.8% | 1.6% | 0.9% | 16.0% | 0.9% | 0.8% | 1.9% | 1.7% | 0.5% | 2.0% | 1.1% |
| *Hyphomicrobium (DEN)* | 1.6% | 0.5% | 0.0% | 0.5% | 0.4% | 0.0% | 1.5% | 0.4% | 0.2% | 0.8% | 0.2% | 0.1% |
| *Candidatus* Competibacter (GAO) | 0.3% | 0.6% | 0.0% | 0.2% | 0.2% | 0.0% | 1.9% | 0.8% | 0.1% | 1.6% | 0.0% | 0.1% |
| *Asprobacter (HET)* | 1.3% | 0.6% | 0.2% | 1.0% | 0.7% | 0.1% | 0.2% | 0.1% | 0.3% | 0.2% | 0.3% | 0.1% |
| *Ferruginibacter (HET)* | 1.0% | 0.7% | 0.0% | 1.2% | 1.0% | 0.0% | 0.6% | 0.3% | 0.3% | 0.5% | 0.2% | 1.3% |
| *Dechloromonas (DPAO)* | 0.3% | 0.2% | 0.0% | 0.8% | 0.3% | 0.0% | 0.2% | 0.5% | 0.1% | 0.0% | 0.0% | 0.1% |
| *Denitratisoma (DEN)* | 0.2% | 0.1% | 0.0% | 0.1% | 0.1% | 0.0% | 0.2% | 0.1% | 0.1% | 0.1% | 0.0% | 0.2% |
| *Thauera (DEN)* | 0.7% | 0.2% | 0.2% | 1.2% | 0.2% | 0.0% | 2.5% | 0.2% | 0.0% | 1.7% | 0.0% | 1.6% |
| *Hydrogenophaga (DEN)* | 0.1% | 0.4% | 3.6% | 0.4% | 4.2% | 0.7% | 0.0% | 5.0% | 7.6% | 0.0% | 5.1% | 5.1% |
| *Zoogloea (DEN and NIT)* | 0.0% | 0.0% | 0.2% | 0.2% | 0.0% | 0.0% | 0.0% | 0.4% | 1.2% | 0.1% | 0.2% | 0.2% |
| *Mycolicibacter (HET)* | 0.2% | 0.2% | 4.6% | 0.1% | 0.1% | 3.2% | 0.6% | 0.2% | 0.3% | 0.4% | 0.4% | 0.1% |
| *Comamonas (HET/DEN???)* | 0.4% | 10.9% | 48.6% | 0.5% | 4.1% | 77.7% | 0.0% | 11.2% | 6.5% | 0.1% | 16.7% | 6.9% |
| *Legionella (HET)* | 0.1% | 0.1% | 3.9% | 0.3% | 0.2% | 0.5% | 0.1% | 0.0% | 0.1% | 0.1% | 0.6% | 0.0% |
| *Simplicispira (DEN)* | 0.0% | 3.7% | 4.1% | 0.1% | 1.0% | 0.0% | 0.0% | 5.0% | 4.9% | 0.0% | 1.5% | 2.5% |
| *Pseudoxanthomonas (DEN/new DPAO???)* | 0.0% | 0.0% | 0.7% | 0.0% | 0.1% | 0.2% | 0.0% | 0.9% | 4.9% | 0.0% | 4.0% | 0.5% |
| *Rhodoferax (DEN)* | 7.5% | 1.9% | 0.1% | 3.7% | 0.9% | 0.0% | 0.0% | 0.2% | 0.0% | 0.2% | 0.2% | 0.1% |
| *Rhodococcus (HET DEN and NIT)* | 0.0% | 0.1% | 0.3% | 0.0% | 0.1% | 0.4% | 0.0% | 0.6% | 4.5% | 0.0% | 13.7% | 8.7% |
| *Rhodobacter (DEN)* | 0.7% | 1.1% | 0.6% | 1.1% | 1.0% | 0.1% | 1.2% | 0.5% | 0.6% | 0.8% | 0.1% | 0.1% |
| *Sphingopyxis (HET)* | 0.0% | 0.0% | 0.3% | 0.0% | 0.1% | 0.2% | 0.0% | 1.3% | 1.4% | 0.0% | 0.8% | 0.6% |
| *Pseudomonas (DEN)* | 0.0% | 1.7% | 0.4% | 0.2% | 2.6% | 0.0% | 0.0% | 0.6% | 2.7% | 0.0% | 14.9% | 3.6% |
| *Brevundimonas (DEN)* | 0.3% | 0.2% | 0.4% | 0.1% | 0.9% | 0.1% | 0.1% | 0.6% | 1.4% | 0.0% | 0.6% | 1.9% |
| *Denitratimonas (DEN)* | 1.1% | 0.6% | 0.2% | 2.4% | 1.0% | 0.0% | 0.0% | 0.1% | 0.2% | 0.1% | 0.5% | 0.9% |
| *Chryseolinea* related *(HET)* | 0.8% | 0.8% | 0.0% | 1.0% | 1.2% | 0.0% | 0.8% | 2.4% | 3.7% | 0.5% | 0.2% | 0.3% |
| *Simplicispira (DEN)* | 0.0% | 3.7% | 4.1% | 0.1% | 1.0% | 0.0% | 0.0% | 5.0% | 4.9% | 0.0% | 1.5% | 2.5% |
| *Bdellovibrio (DEN predator)* | 0.4% | 0.2% | 0.2% | 0.4% | 0.5% | 0.0% | 0.3% | 0.5% | 0.3% | 0.3% | 0.4% | 3.3% |
| *Ferruginibacter (DEN)* | 1.0% | 0.7% | 0.0% | 1.2% | 1.0% | 0.0% | 0.6% | 0.3% | 0.3% | 0.5% | 0.2% | 1.3% |
| *Glutamicibacter (HET)* | 0.0% | 0.0% | 0.0% | 0.0% | 0.0% | 0.0% | 0.0% | 0.0% | 0.0% | 0.5% | 0.2% | 1.3% |

| | | | | | | | | | | | | |
|---|---|---|---|---|---|---|---|---|---|---|---|---|
| *Flavobacterium (DEN)* | 0.2% | 0.2% | 0.1% | 0.5% | 0.3% | 0.1% | 0.2% | 0.4% | 2.3% | 0.3% | 0.3% | 3.1% |
| *TOTAL:* | **62.9%** | **66.3%** | **79.6%** | **58.0%** | **76.3%** | **86.3%** | **41.8%** | **63.3%** | **69.5%** | **40.7%** | **63.9%** | **73.7%** |

840

841 ## S3. Initial biomass concentrations for simulation of the long-term experiments

842 **Table S3**. Initial biomass concentrations for simulation of the long-term experiments

| Parameters | Units | Initial biomass concentration | | | |
|---|---|---|---|---|---|
| | | T1 | T2 | T3 | T4 |
| $X_{AOB}$ | mg COD/L | 36.4 | 34.3 | 0 | 0 |
| $X_{NOB1}$ | mg COD/L | 13 | 12.5 | 11.5 | 11 |
| $X_{NOB2}$ | mg COD/L | 0.13 | 0.12 | 0.11 | 0.11 |
| $X_{CMX}$ | mg COD/L | 4.8 | 6.0 | 4.5 | 4.0 |
| $X_{HET}$ | mg COD/L | 380 | 405 | 385 | 390 |

843

844

## S4. Review on stochiometric and kinetic parameters

**Table S4**. Review of recent literature data on the stoichiometric and kinetic parameters related to the specific groups of canonical AOB (r-AOB vs. K-AOB), canonical NOB (r-NOB vs. K-NOB), and comammox bacteria

| Parameters (Unit) | Canonical r-AOB (*Nitrosomonas*) | Canonical K-AOB (*Nitrosospira*) | Canonical r-NOB (*Nitrospira*) | Canonical K-NOB (*Nitrobacter*) | Comammox (*Nitrospira)* | References |
|---|---|---|---|---|---|---|
| $\mu_{max}$ ($d^{-1}$) | 0.24 | | 0.18 | | | (Liu and Wang 2014) |
| | 0.2-0.9 | | | | | (Metcalf et al., 2003) |
| | 3.03 | 1.01 | 0.93 | 0.31 | | (Yu et al., 2020) |
| | 0.54-2.1 | 0.7-0.9 | | | | (Zhang et al., 2019) |
| | | | 0.39-1.28 | | 0.69 | (Park et al., 2017) |
| | 0.94–0.99 | | 2.25–2.51 | | | (Liu et al., 2017) |
| b ($d^{-1}$) | 0.09–0.27 | | 0.09–0.27 | | | (Metcalf et al., 2003) |
| | 0.05-0.15 | | 0.05-0.15 | | | (Henze 2000) |
| $K_{NH4}$ (mg N/L) | 0.675 | 0.225 | | | | (Yu et al., 2020) |
| | | | | | 0.0005 | (Sakoula et al., 2021) |
| | | | | | 0.012 | (Koch et al., 2019) |
| | 0.076-0.612 | | | | 0.009 | (Kits et al., 2017) |
| $K_{NO2}$ (mg N/L) | | | 0.765 | 0.255 | | (Yu et al., 2020) |
| | | | | | 0.175 | (Sakoula et al., 2021) |
| | | | | 0.084-0.378 | 6.29 | (Koch et al., 2019) |
| | | | 0.3-7.6 | 0.1-1.1 | | (Park et al., 2017) |
| | - | - | 0.69-7.62 | 0.126-0.378 | 5.21 | (Nowka et al., 2015) |
| $K_O$ (mg $O_2$/L) | 0.42 | 0.14 | 1.35 | 0.45 | | (Yu et al., 2020) |
| | 0.15-1.15 | | 0.13-1.10 | | | (Zhang et al., 2019) |
| | | | 0.17-4.32 | | 0.33 | (Park et al., 2017) |
| | 0.36 | | 0.54 | | | (Liu et al., 2017) |
| Y (mg COD/mg N) | 0.18 | | 0.08 | | | (Jubany et al., 2008) |
| | | | 0.07-0.14 | | | (Park et al., 2017) |
| | | | | | 0.2-0.38 | (Kits et al., 2017) |
| | 0.15-0.24 | | | | | (Eldyasti et al., 2012) |

μ: maximum specific growth rate, K: half-saturation coefficient, b: decay coefficient, Y: growth yield coefficient

850

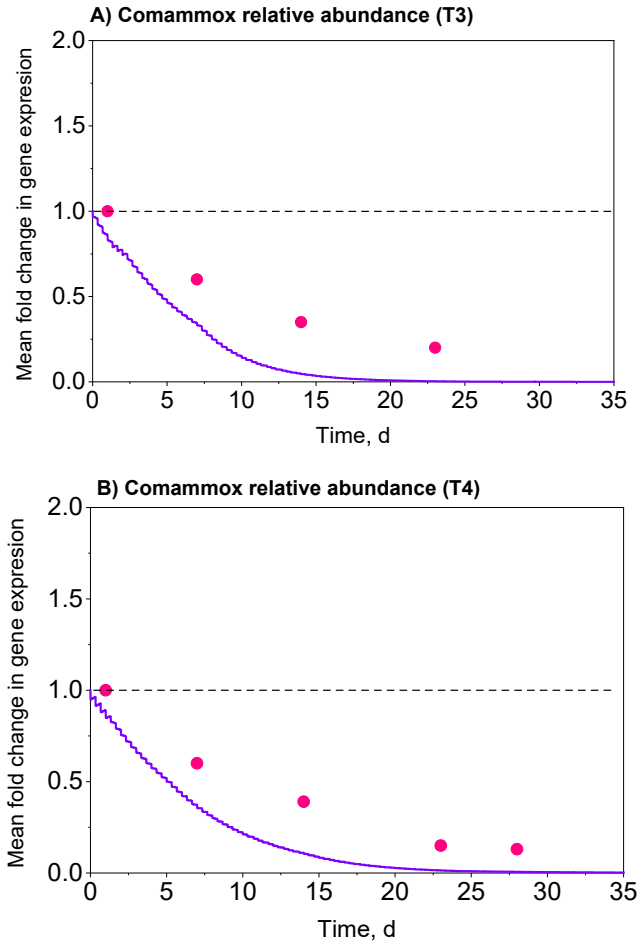


851
852 **Figure S2-** Observed vs. predicted relative adundances of comammox bacteria in trial T3 (comammox can growth
853 only on $NH_4$-N)
854
855

856 **Table S5**. Kinetic and stoichiometric parameters for canonical *Nitrospira*, comammox *Nitrospira*, and *Nitrobacter*
857 reported in the literature

| Bacteria | $\mu_{max}$ ($d^{-1}$) | b ($d^{-1}$) | Y (g VSS/g N or g COD/g N) | $K_{NH4}$ (mg N/L) | $K_{NO2}$ (mg N/L) | $K_O$ (mg $O_2$/L) | Remarks | Reference |
|---|---|---|---|---|---|---|---|---|
| *Nitrospira* | | | | | | | | |
| | 0.31 | 0.02 | - | | 0.25 | 0.45 | T= 17-22 °C, pH=7.5–8.2, Enriched culture | (Yu et al., 2020) |
| | 0.69 ± 0.10 | - | 0.14 ± 0.02 (g VSS/g N) | - | 0.52 ± 0.14 | 0.33 ± 0.04 | T=22 °C, pH=7.5±0.1 Enriched culture, lineage I | (Park et al. 2017) |
| | | | 0.12 ± 0.04 (g VSS/g N) | - | 0.9-1.1 | 0.54 | T=22 °C, pH=7.5 Enriched culture | (Blackburne et al. 2007) |
| | 0.45-0.52 | - | - | - | 0.13-0.39 | - | T=28–37 °C, pH=7.4-8.6 Pure culture, *Nitrospira* defluvii, and Moscoviensis, | (Nowka et al. 2015) |
| | - | | - | - | 0.08 (Lineage I) 0.14 (Lineage II) | - | T=29°C, Pure culture, *Nitrospira* lineage I and II | (Ushiki et al. 2017) |
| | 0.45 | - | - | - | - | - | T=N/a, Enriched culture | (Lawson and Lücker 2018) |
| | - | - | - | - | 5.21 | - | T=37 °C, Pure culture, *clade 1, lineage II* | (Kits et al. 2017) |

| | | | | | | | | |
|---|---|---|---|---|---|---|---|---|
| | 0.2 | 0.04 | 0.05<br>(g COD/g N) | | 0.06 | 0.13 | T=12-20 °C,<br>Mixed culture | This study |

858

| | | | | | | | | |
|---|---|---|---|---|---|---|---|---|
| Comammox -*Nitrospira* | 0.148 | - | - | 0.009 | - | - | T=N/a, Enriched culture Clade A | (Lawson and Lücker, 2018) |
| | - | | - | 0.012 | 6.29 | - | T= NA, pH= NA Pure culture, *lineage II* | (Koch et al. 2019) |
| | | | | 0.0005 | 0.175 | | | (Sakoula et al., 2021) |
| | 0.2 | 0.04 | 0.15 (g COD/g N) | - | - | - | T=12-20 °C, Mixed culture Clade A | This study |
| *Nitrobacter* | 0.93 | 0.05 | | | 0.76 | 1.35 | T= 17-22 °C, pH=7.5–8.2, Enriched culture | (Yu et al., 2020) |
| | - | | 0.08 (g VSS/g N) | - | 1.2−1.3 | 0.43 | T=22 °C, Enriched culture, | (Blackburne et al., 2007) |
| | 0.39−1.28 | - | - | - | 0.69−7.6 | - | T= 28–37 °C pH=7.4-8.6, Pure culture | (Nowka et al., 2015) |
| | - | | - | - | - | 0.17−4.32 | T=25 °C, pH=7.3-8.2, Pure culture | (Laanbroek et al., 1994) |
| | 0.48 | | 0.07−0.1 (g VSS/g N) | - | 1.49 | - | T=22 °C, pH=7.3, Mixed culture | (Vadivelu et al., 2006) |
| | 0.6 | 0.08 | 0.05 (g COD/g N) | | 0.06 | 0.45 | | This study |

859 $\mu_{max}$: Maximum growth rate, Y: Yield coefficient, Ko: DO affinity constant, $K_{NH4}$: Ammonia affinity constant, $K_{NO2}$:
860 Nitrite affinity constant,
861

862

## References


Blackburne R, Vadivelu VM, Yuan Z, Keller J. Kinetic characterisation of an enriched Nitrospira culture with comparison to Nitrobacter. Water Research 2007; 41: 3033-3042.

Eldyasti, A., Nakhla, G. and Zhu, J., 2012. Development of a calibration protocol and identification of the most sensitive parameters for the particulate biofilm models used in biological wastewater treatment. Bioresource Technology 111, 111-121. 10.1016/j.biortech.2012.02.021

Henze, M.G., W., Mino, T., van Loosdrecht, M.C.M. (2000) Activated sludge models ASM1, ASM2, ASM2d and ASM3, IWA Publishing, London, UK.

Jubany, I., Carrera, J., Lafuente, J. and Baeza, J.A., 2008. Start-up of a nitrification system with automatic control to treat highly concentrated ammonium wastewater: Experimental results and modeling. Chemical Engineering Journal 144(3), 407-419. 10.1016/j.cej.2008.02.010

Kits, K.D., Sedlacek, C.J., Lebedeva, E.V., Han, P., Bulaev, A., Pjevac, P., Daebeler, A., Romano, S., Albertsen, M., Stein, L.Y., Daims, H. and Wagner, M., 2017. Kinetic analysis of a complete nitrifier reveals an oligotrophic lifestyle. Nature 549(7671), 269-272. 10.1038/nature23679

Koch, H., van Kessel, M.A.H.J. and Lücker, S., 2019. Complete nitrification: insights into the ecophysiology of comammox Nitrospira. Applied Microbiology and Biotechnology 103(1), 177-189. 10.1007/s00253-018-9486-3

Klindworth, A., Pruesse, E., Schweer, T., Peplies, J., Quast, C., Horn, M. and Glöckner, F.O., 2012. Evaluation of general 16S ribosomal RNA gene PCR primers for classical and next-generation sequencing-based diversity studies. Nucleic Acids Research 41(1), e1-e1. 10.1093/nar/gks808

Liu, G. and Wang, J., 2014. Role of Solids Retention Time on Complete Nitrification: Mechanistic Understanding and Modeling. Journal of Environmental Engineering 140(1), 48-56. 10.1061/(ASCE)EE.1943-7870.0000779

Meyer, F., Paarmann, D., D'Souza, M., Olson, R., Glass, E.M., Kubal, M., Paczian, T., Rodriguez, A., Stevens, R., Wilke, A., Wilkening, J. and Edwards, R.A., 2008. The metagenomics RAST server – a public resource for the automatic phylogenetic and functional analysis of metagenomes. BMC Bioinformatics 9(1), 386-399. 10.1186/1471-2105-9-386

Laanbroek HJ, Bodelier PLE, Gerards S. Oxygen consumption kinetics of Nitrosomonas europaea and Nitrobacter hamburgensis grown in mixed continuous cultures at different oxygen concentrations. Archives of Microbiology 1994; 161: 156-162.

Lawson CE, Lücker S. Complete ammonia oxidation: an important control on nitrification in engineered ecosystems? Current Opinion in Biotechnology 2018; 50: 158-165.

Liu, J., Wu, Y., Wu, C., Muylaert, K., Vyverman, W., Yu, H.-Q., Muñoz, R. and Rittmann, B., 2017. Advanced nutrient removal from surface water by a consortium of attached microalgae and bacteria: A review. Bioresource Technology 241, 1127-1137. 10.1016/j.biortech.2017.06.054

Metcalf and Eddy, Inc. 2003. Wastewater engineering : treatment and reuse, Fourth edition / revised by George Tchobanoglous, Franklin L. Burton, H. David Stensel. Boston : McGraw-Hill, 2003.

Nowka, B., Daims, H. and Spieck, E., 2015. Comparison of Oxidation Kinetics of Nitrite-Oxidizing Bacteria: Nitrite Availability as a Key Factor in Niche Differentiation. Applied and Environmental Microbiology 81(2), 745. 10.1128/AEM.02734-14

Park, M.-R., Park, H. and Chandran, K., 2017. Molecular and Kinetic Characterization of Planktonic Nitrospira spp. Selectively Enriched from Activated Sludge. Environmental Science & Technology 51(5), 2720-2728. 10.1021/acs.est.6b05184

Pjevac, P., Schauberger, C., Poghosyan, L., Herbold, C.W., van Kessel, M.A.H.J., Daebeler, A., Steinberger, M., Jetten, M.S.M., Lücker, S., Wagner, M. and Daims, H., 2017. AmoA-Targeted Polymerase Chain Reaction Primers for the Specific Detection and Quantification of Comammox Nitrospira in the Environment. Frontiers in Microbiology 8(1508). 10.3389/fmicb.2017.01508

Sakoula, D., Koch, H., Frank, J., Jetten, M.S.M., van Kessel, M.A.H.J. and Lücker, S., 2021. Enrichment and physiological characterization of a novel comammox Nitrospira indicates ammonium inhibition of complete nitrification. The Isme Journal 15(4), 1010-1024. 10.1038/s41396-020-00827-4

Vadivelu VM, Yuan Z, Fux C, Keller J. 2006. Stoichiometric and kinetic characterisation of Nitrobacter in mixed culture by decoupling the growth and energy generation processes. Biotechnology and Bioengineering 94: 1176-1188.

Yu, L., Chen, S., Chen, W. and Wu, J., 2020. Experimental investigation and mathematical modeling of the competition among the fast-growing “r-strategists” and the slow-growing “K-strategists” ammonium-oxidizing bacteria and nitrite-oxidizing bacteria in nitrification. Science of The Total Environment 702, 135049. 10.1016/j.scitotenv.2019.135049

Zhang, D., Su, H., Antwi, P., Xiao, L., Liu, Z. and Li, J., 2019. High-rate partial-nitritation and efficient nitrifying bacteria enrichment/out-selection via pH-DO controls: Efficiency, kinetics, and microbial community dynamics. Science of The Total Environment 692, 741-755. 10.1016/j.scitotenv.2019.07.308